Science Translational Medicine
AAAS

Supplementary Materials for

Deleting DNMT3A in CAR T cells prevents exhaustion and enhances antitumor activity

Brooke Prinzing *et al.*

Corresponding author: Giedre Krenciute, giedre.krenciute@stjude.org; Ben Youngblood, benjamin.youngblood@stjude.org; Stephen Gottschalk, stephen.gottschalk@stjude.org

Sci. Transl. Med. **13**, eabh0272 (2021)
DOI: 10.1126/scitranslmed.abh0272

The PDF file includes:

Figs. S1 to S30
Table S1

Other Supplementary Material for this manuscript includes the following:

Data files S1 and S2

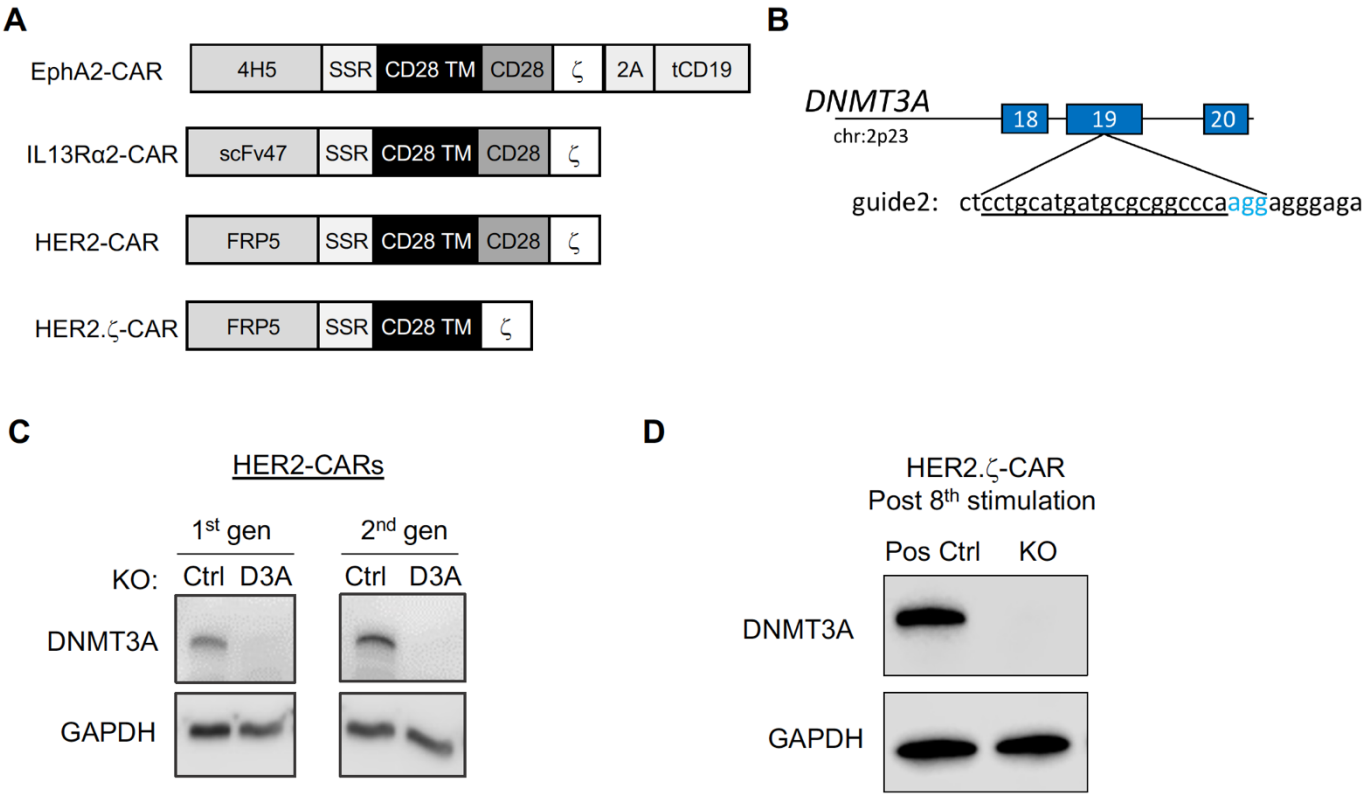

Fig. S1. Chimeric antigen receptor (CAR) design, guide RNA, and editing efficiencies. (**A**) The schemes of ephrin type-A receptor 2 (EphA2), human epidermal growth factor receptor 2 (HER2) and interleukin 13 receptor subunit alpha 2 (IL13Rα2)-specific CAR retroviral vectors are shown. SSR: short spacer region; (**B**) The schematic shows the Cas9/guide (g)RNA target site for DNA methyltransferase 3 alpha (DNMT3A). The gRNA target sequence is underlined, and the protospacer adjacent motif (PAM) sequence is labeled in blue. Numbers in the blue boxes indicate DNMT3A exons. (**C**) Western blot analysis of DNMT3A expression in control (Ctrl) knockout (KO) and DNMT3A KO HER2-specific 1st and 2nd generation CAR T cells is shown. GAPDH was used as a loading control. (**D**) HER2.ζ-CAR T cells were repeatedly stimulated with tumor cells as described in **Fig. 1C**. After the 8th stimulation with tumor cells, DNMT3A KO CAR T cells were collected for western blot analysis to ensure long-term stability of the KO. GAPDH was used as a loading control. As Ctrl KO CAR T cells had crashed by this time point, unmodified T cells were used as a positive control for DNMT3A expression (Pos Ctrl).

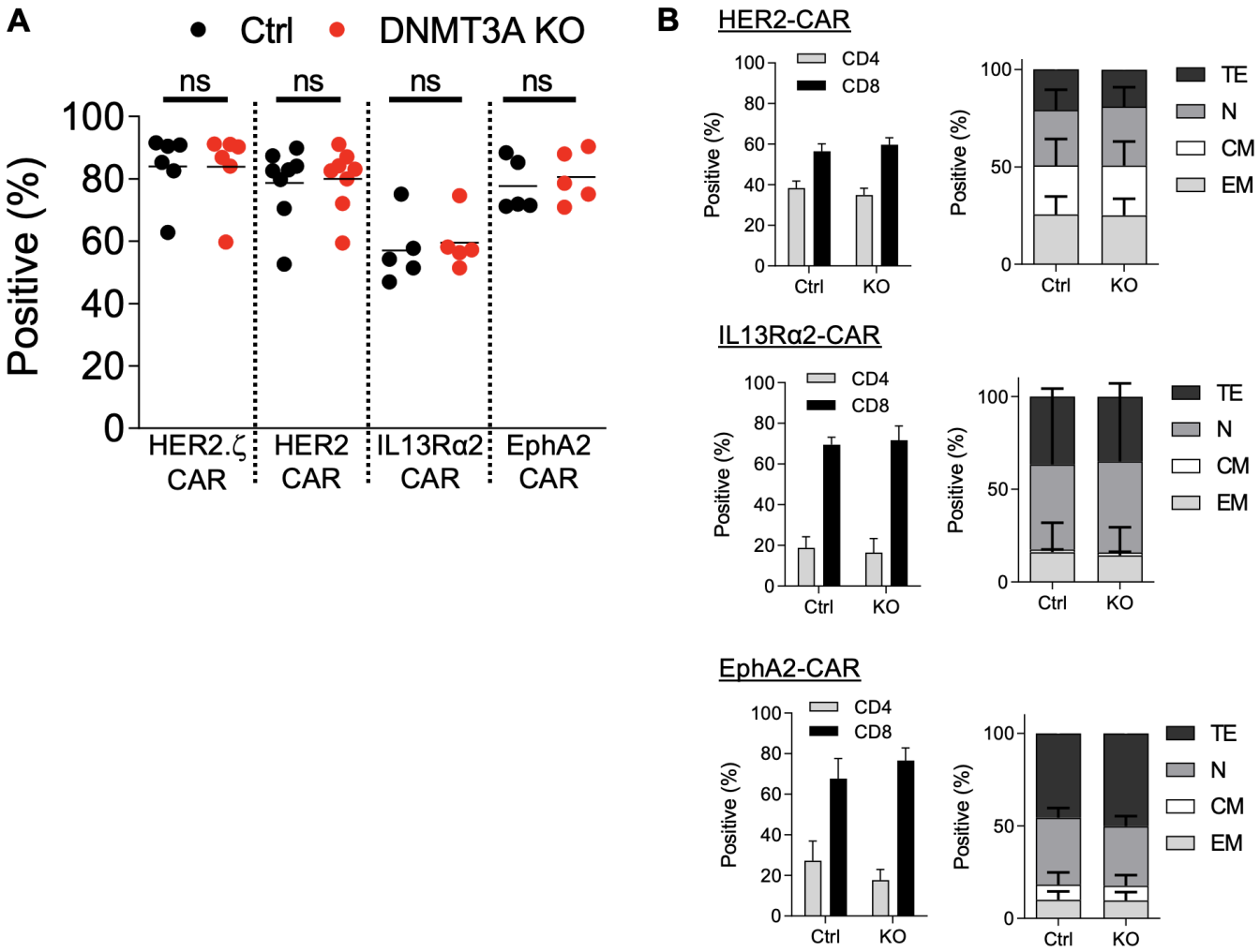

Fig. S2. CAR expression and phenotype. (**A**) Summary data for CAR expression in gene edited CAR T cells was determined using flow cytometry analysis (n=5 to 8 per CAR; one-way ANOVA with Bonferroni's multiple comparisons test, ns=not significant). Horizontal bars indicate mean. (**B**) CAR T cell phenotype was evaluated before stimulation with tumor cells (day 10 to 12 post-transduction, n=2 to 3 per CAR construct). TE, terminal effector ($CCR7^{-}CD45RO^{-}$), N, naïve ($CCR7^{+}CD45RO^{-}$), EM, effector memory ($CCR7^{-}CD45RO^{+}$), CM, central memory ($CCR7^{+}CD45RO^{+}$). Data are presented as mean+SEM.

A

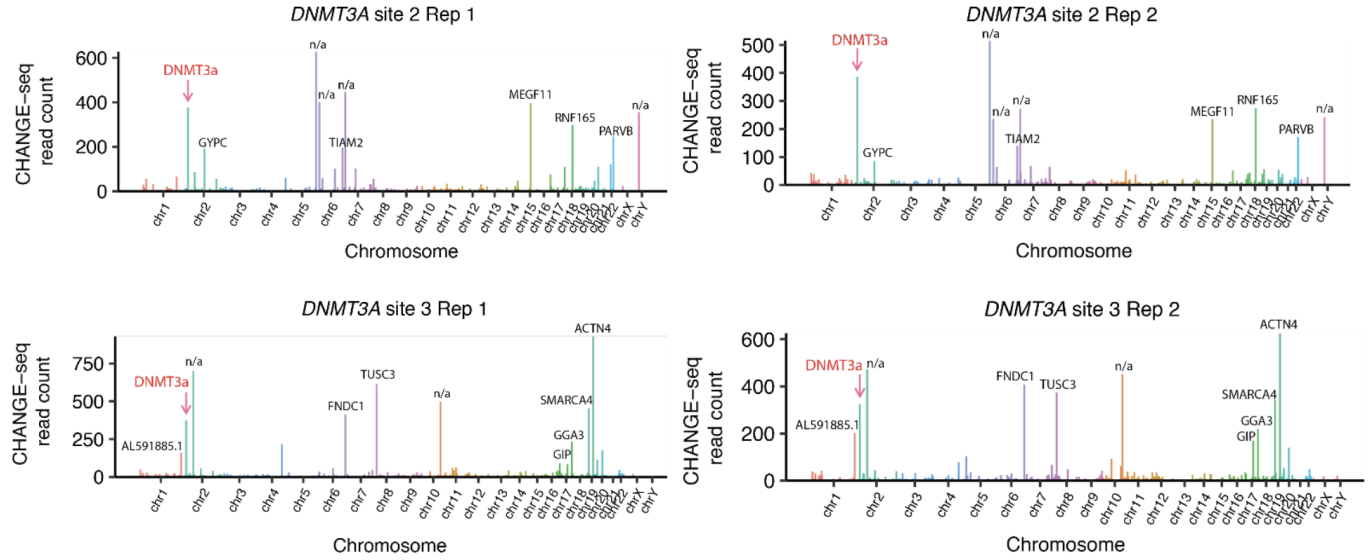

B

guide 2											
Chromosome	**Start**	**End**	**Summary**	**Strand**	**Offtarget**	**Distance**	**repeat 1**	**repeat 2**	**Target gene**		
5	175166512	175166535	5:175166512-175166535	-	TTGGCATGATGCACGGCCCATGA	5	628	516	n/a		
2	**25240390**	**25240413**	**2:25240390-25240413**	**-**	**CCTGCATGATGCGCGGCCCAAGG**	**0**	**376**	**386**	**DNMT3A**	**exon 19**	Intended target
18	46359193	46359216	18:46359193-46359216	+	TCTGCATGATGCCAGGCCCAGGG	3	298	274	RNF165	intron	
7	1371396	1371419	7:1371396-1371419	-	CCTGCATGGTGCCCGACCCAGGG	3	448	272	n/a		
X	148335014	148335037	X:148335014-148335037	+	TTTGCATGATATGCAGCCCAAGG	5	356	242	n/a		
6	14515851	14515874	6:14515851-14515874	+	GCTCCATGATGCACGGCCCAGGG	3	402	236	n/a		
15	66101615	66101638	15:66101615-66101638	+	CTAGCATGATGCCCGGCACATGG	4	396	234	MEGF11	intron	
22	44086193	44086215	22:44086193-44086215	-	CATGCAGGATGC-CGGCCCAGGG	3	246	170	PARVB	intron	
6	155137732	155137754	6:155137732-155137754	-	TCTGCATGAAG-GCAGCCCATGG	4	196	140	TIAM2	intron	
2	126664841	126664863	2:126664841-126664863	-	CCTGCA-GATGCCCAGCCCAGGG	3	192	86	GYPC	intron	
guide 3											
Chromosome	**Start**	**End**	**Summary**	**Strand**	**Offtarget**	**Distance**	**repeat 1**	**repeat 2**	**Target gene**		
19	38724865	38724888	19:38724865-38724888	+	TGATGGTGCGCAGCCCAAGGAGG	4	928	626	ACTN4	intron	
2	66820696	66820719	2:66820696-66820719	-	GCATCATGCACAGCCCAAGGAGG	3	702	472	n/a		
10	111130701	111130724	10:111130701-111130724	-	GCAGGATGCACATCCCAAGGTGG	4	496	452	n/a		
6	159195324	159195347	6:159195324-159195347	+	TGAGGATGCGCAGCCCAAGGTGA	5	412	408	FNDC1	intron 1	
8	15715486	15715509	8:15715486-15715509	+	GCATGATTCGCAGCCCAAGGAGG	2	614	374	TUSC3	intron 6	
19	10977204	10977227	19:10977204-10977227	+	ACCTGATGCGCGCCCAAGAGGGG	6	454	342	SMARCA4	intron 1	
2	**25240387**	**25240410**	**2:25240387-25240410**	**-**	**GCATGATGCGCGGCCCAAGGAGG**	**0**	**374**	**326**	**DNMT3A**	**exon 19**	Intended target
17	75237836	75237859	17:75237836-75237859	-	GACAGATGCACGGCCCAAGGGGC	5	234	220	GGA3	exon 17	
1	244008378	244008401	1:244008378-244008401	+	GACAAATGCGCAGCCCAAGATGG	6	160	202	AL591885.	intron 4	
17	48964196	48964219	17:48964196-48964219	-	ACATGATGCACAACCCCAGGTGG	5	84	170	GIP	intron 3	

Fig. S3. gRNA off-target screen using circularization for high-throughput analysis of nuclease genome-wide effects by sequencing (CHANGE-seq). (**A**) Manhattan plots showing genome wide targeting specificity of Cas9 to DNMT3A sites 2 and 3. (**B**) List of top 10 evaluated genes known to be off-targets of DNMT3A-targeting guide RNAs.

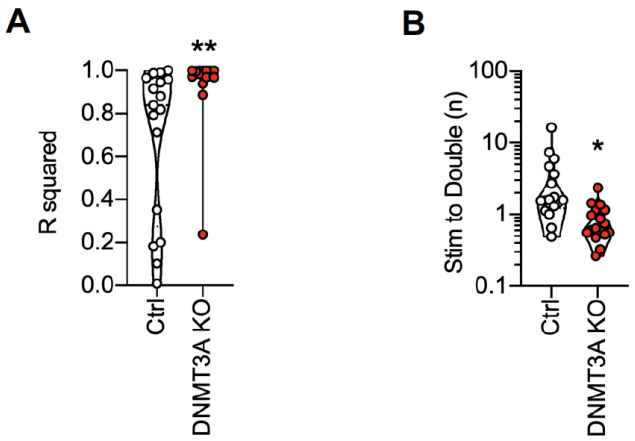

Fig. S4. The expansion of DNMT3A KO CAR T cells post repeat stimulations follows an exponential growth pattern. CAR T cell expansion (n=17 each for Ctrl and DNMT3A KO CAR T cells) from **Fig. 1D** was analyzed using an exponential (Malthusian) growth model. (**A**) R squared of individual fitted growth curves are shown; data were analyzed using a paired t-test. **p<0.01 for Ctrl versus DNMT3A KO CAR T cells. (**B**) Number of stimulations needed to achieve CAR T cell doubling [Stim to Double (n)] is shown based on the fitted growth curves; data were analyzed using a paired t-test. *p<0.05 for Ctrl versus DNMT3A KO CAR T cells. Data is presented as truncated Violin plots (minimum to maximum value) with all data points shown.

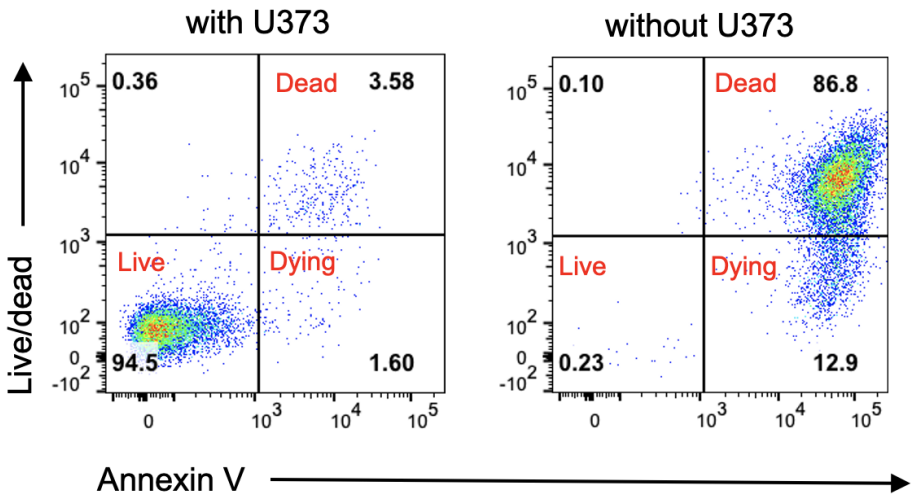

Fig. S5. DNMT3A KO CAR T cells remain antigen-dependent for survival. Data accompanies **Fig. 1F**. After the 4th stimulation with tumor cells, DNMT3A KO HER.ζ or HER2.CD28ζ CAR T cells were sorted and plated with or without antigen (U373 tumor cells) in the presence or absence of interleukin (IL)-15. After 7 days, the proportions of dead, dying, and live T cells were determined by flow cytometry. Representative flow cytometry pots are shown.

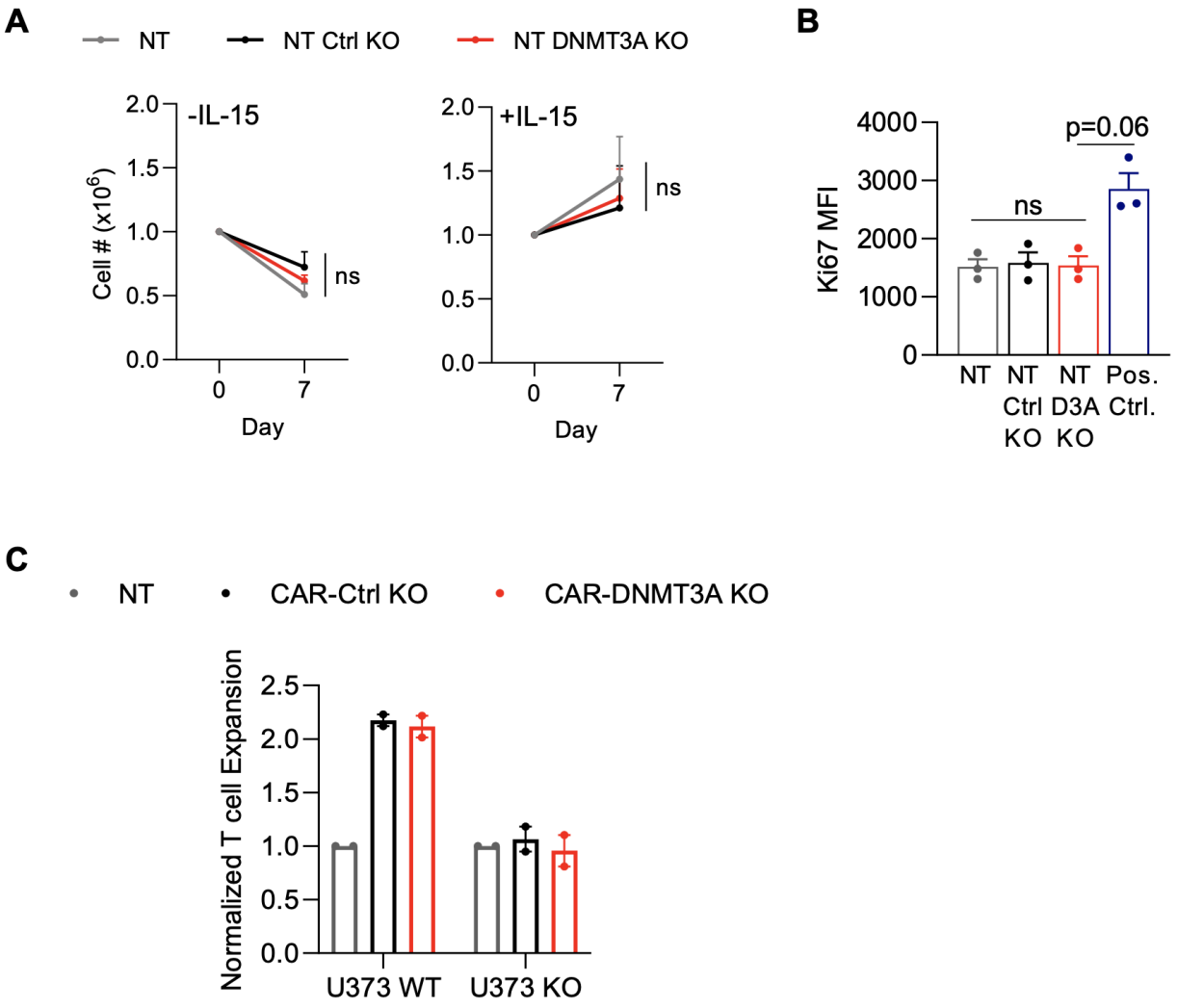

Fig. S6. Deletion of DNMT3A does not enhance alloreactivity nor obviate the antigen-dependence of CAR T cells. (**A and B**) Non-transduced T cells (NT) were electroporated with Cas9 and sgRNA targeting mCherry (Ctrl KO) or DNMT3A (D3A KO). Unmodified non-transduced T cells (NT) were used as a negative control. (**A**) $1x10^6$ T cells were co-cultured with U373 at a 2:1 ratio with or without exogenous IL-15 for 7 days, at which time T cells were gently resuspended and counted with a hemocytometer using Trypan Blue exclusion (n=3, Kruskal-Wallis with Dunn's multiple comparisons test). Data are presented as mean+SEM. (**B**) T cells were co-cultured with U373 + IL-15 as described in (**A**) for 3 days before being evaluated for Ki67 expression using flow cytometry (n=3, Kruskal-Wallis with Dunn's multiple comparisons test). HER2.ζ CAR T cells were used as a positive control (Pos. Ctrl). Data are presented as mean+SEM. MFI indicates mean fluorescence intensity. (**C**) Cocultures were performed with U373 + IL-15 as described in (**A**) using IL13Rα2.CD28ζ CAR T cells and U373 WT or U373 IL13Rα2 KO tumor cells. Expansion is shown relative to NT T cells (n=2); Data are presented as mean±SEM. ns, not significant.

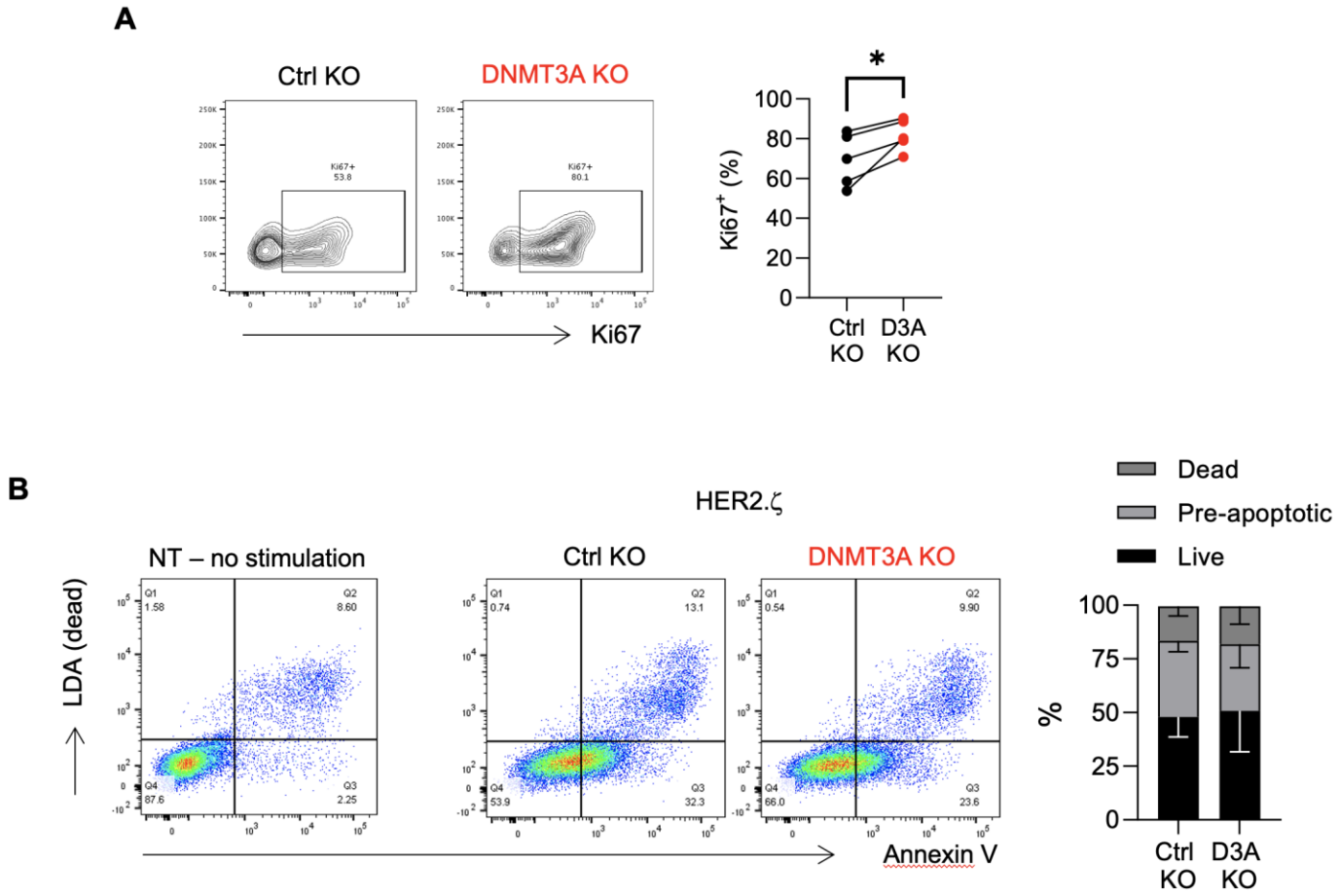

Fig. S7. DNMT3A KO CAR T cells are more proliferative post-stimulation. (A and B) HER2.ζ Ctrl KO or DNMT3A KO CAR cells were used in a repeat stimulation assay against U373 + IL-15 as described in **Fig. 1C**. The analyses shown here were performed after the 4th stimulation with tumor cells. (**A**) Ki67 expression was assessed 24 hours post-stimulation with tumor cells. Representative flow plots and summary data are shown (n=5, paired t-test, *p<0.05). (**B**) T cells were stained with a viability dye (LDA: LIVE/DEAD Aqua) and Annexin V three days post-stimulation with tumor cells. Representative flow plots and summary data are shown. T cells were categorized as live (LDA^-, Annexin V^-), pre-apoptotic (LDA^-, Annexin V^+), or dead (LDA^+, Annexin V^+); Data are presented as mean+SEM (n=3). Data were analyzed using a two-way ANOVA with Sidak's test for multiple comparisons; no significant difference was observed).

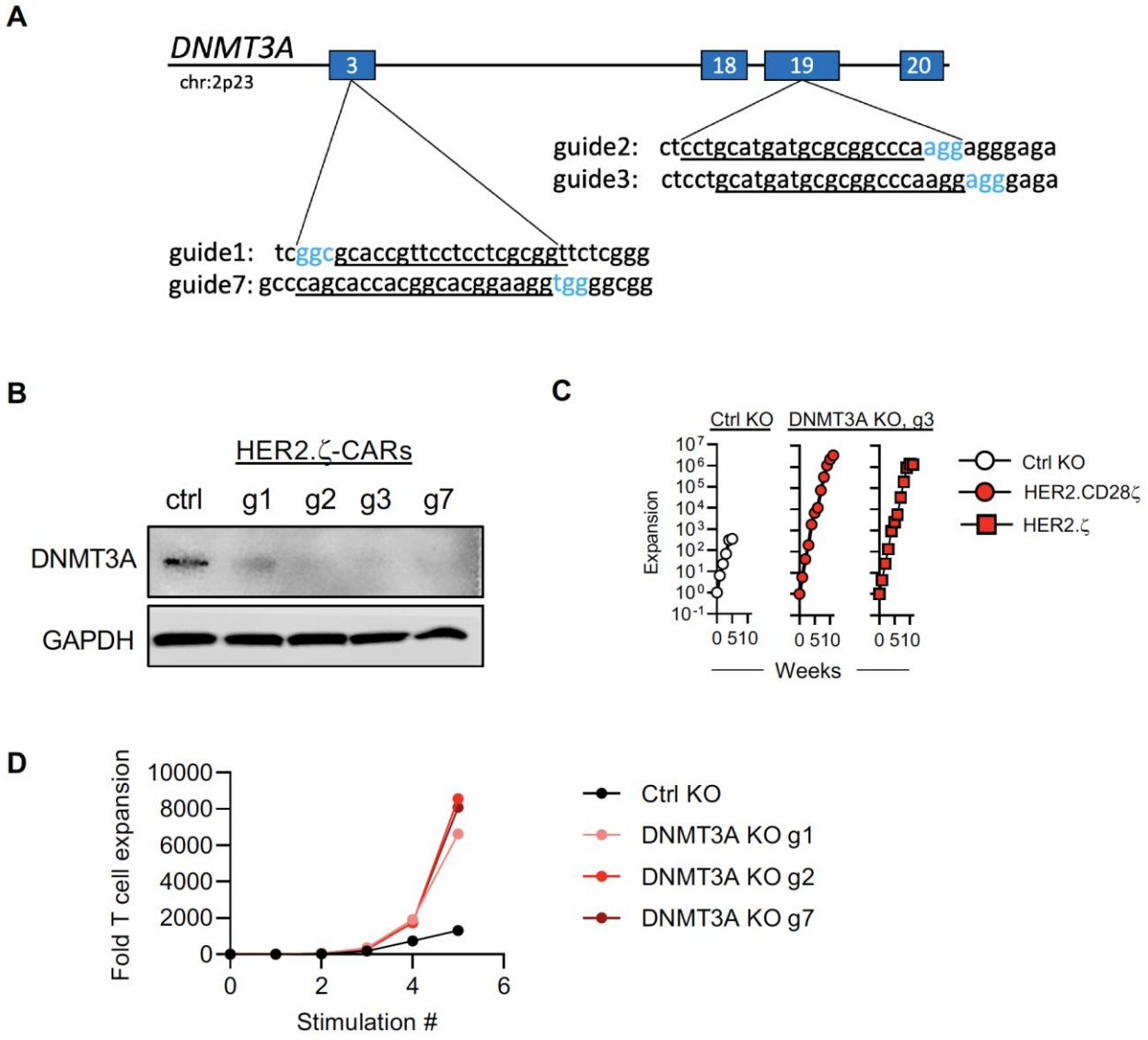

Fig. S8. Silencing DNMT3A with different guide RNAs shows the same improved proliferative capacity. (**A**) Schematic of the Cas9/gRNA target sites for DNMT3A. The gRNA target sequences for guides 1 (g1), 2 (g2), 3 (g3) and 7 (g7) are underlined, and the PAM sequences are labeled in blue. Numbers in the blue boxes indicate DNMT3A exons. (**B**) Western blot analysis of DNMT3A expression in control KO (Ctrl) and DNMT3A-KO HER2.ζ CAR T cells. Four guide RNAs targeting DNMT3A were tested. GAPDH was used as a loading control. (**C**) An alternative sgRNA, guide 3, was used to silence DNMT3A in HER2.CD28ζ (red circles) and HER2.ζ-CAR (red squares) T cells. A repeated stimulation experiment was set up as described in Fig. 1C with HER2.CD28ζ used as Ctrl KO cells (white circles). The assay was carried out until CAR T cells stop killing at which point co-cultures were terminated; n=1 per CAR construct. (**D**) DNMT3A was deleted in HER2.ζ-CAR T cells using 3 different guide RNAs. A repeated stimulation experiment was set up as described in Fig. 1C with HER2.ζ used as Ctrl KO cells; n=1 per CAR construct.

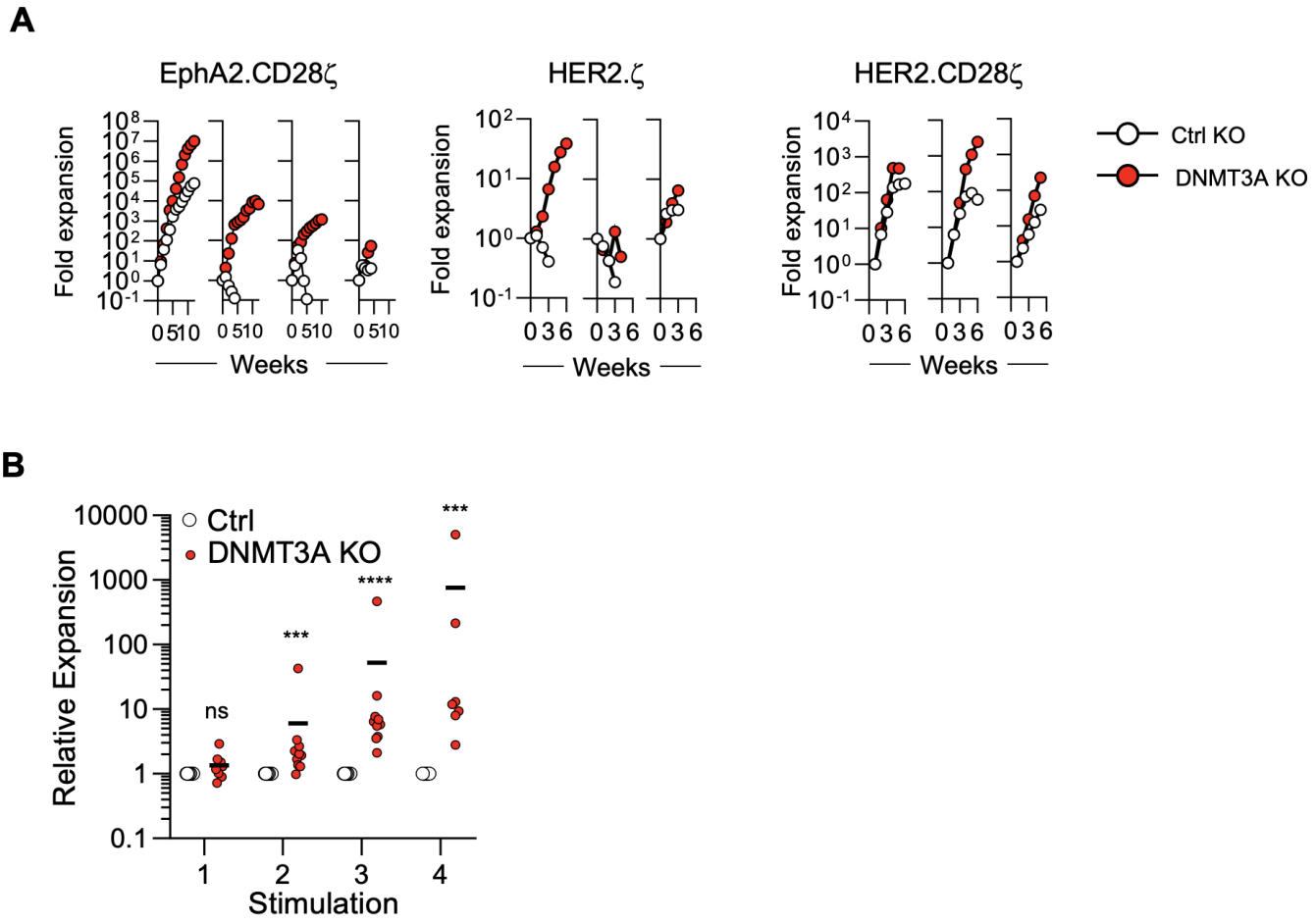

Fig. S9. Deletion of DNMT3A in CAR T cells enhances proliferation in a repeat stimulation assay against LM7 cells. Ctrl and DNMT3A KO EphA2.CD28ζ-, HER2.ζ-, and HER2.CD28ζ-CAR T cells were used in a repeated stimulation assay as described in Fig. 1C against the osteosarcoma cell line LM7. (**A**) Fold T cell expansion for each donor is shown. (**B**) Expansion of DNMT3A KO relative to Ctrl CAR T cells is shown at each of the first four stimulations (n=10, Mann-Whitney tests with two-stage step-up Benjamini, Krieger, & Yekutieli False Discovery Rate procedure, ns: not significant, ***p<0.001, ****p<0.0001). Horizontal bars represent mean.

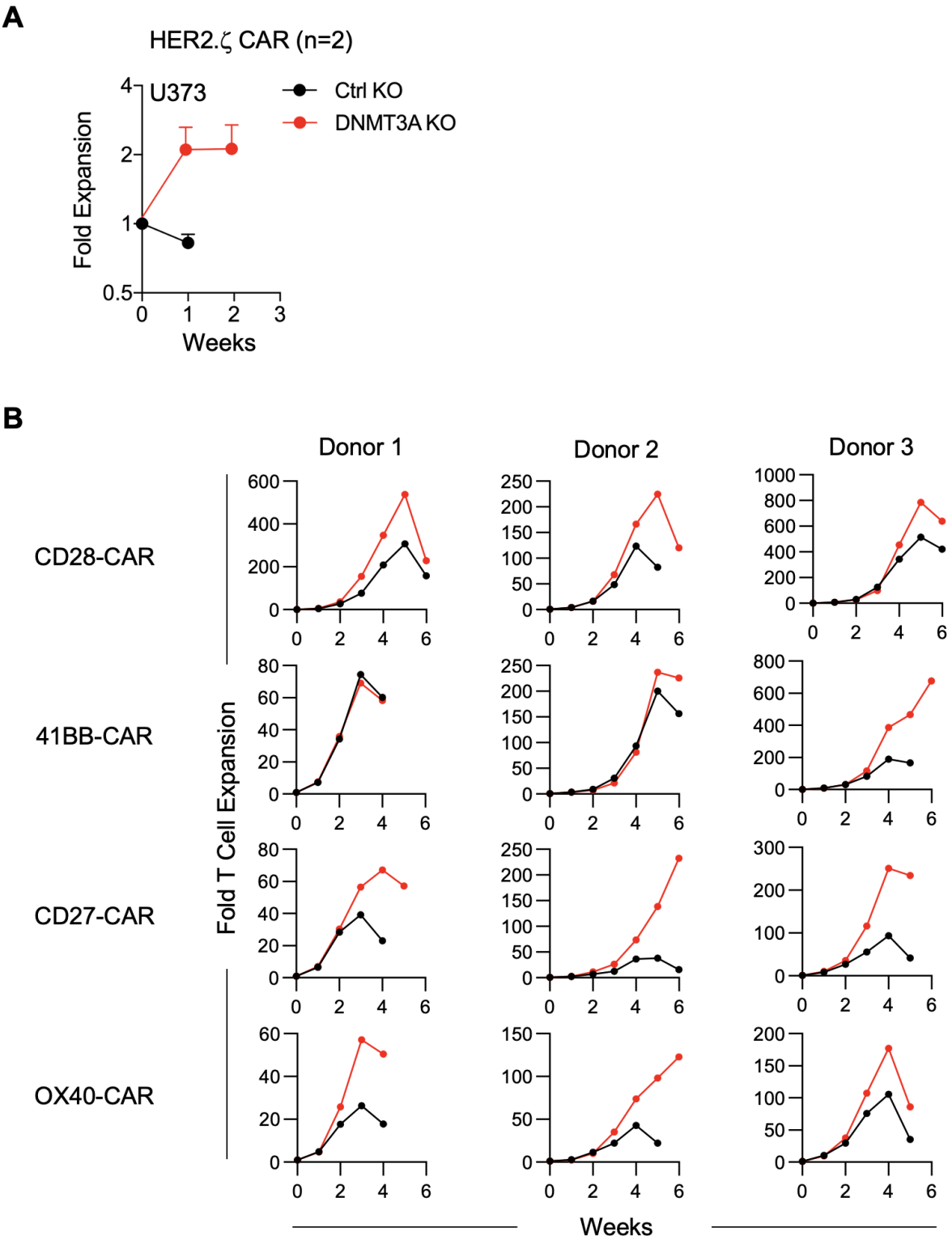

Fig. S10. Repeat stimulation assays of DNMT3A KO and Ctrl KO CAR T cells without IL-15. (**A**) HER2.ζ CAR T cells were co-cultured with U373 tumor cells at a 2:1 ratio in the absence of exogenous IL-15. Every 7 days, T cells were counted and plated on fresh tumor cells until the T cells stopped killing or expanding. Fold T cell expansion is shown. Data are presented as mean+SEM. (**B**) EphA2 CAR T cells with a CD28-, 41BB-, CD27-, or OX40-costimulatory domain were repeatedly stimulated as described in (**A**) and fold expansion was measured.

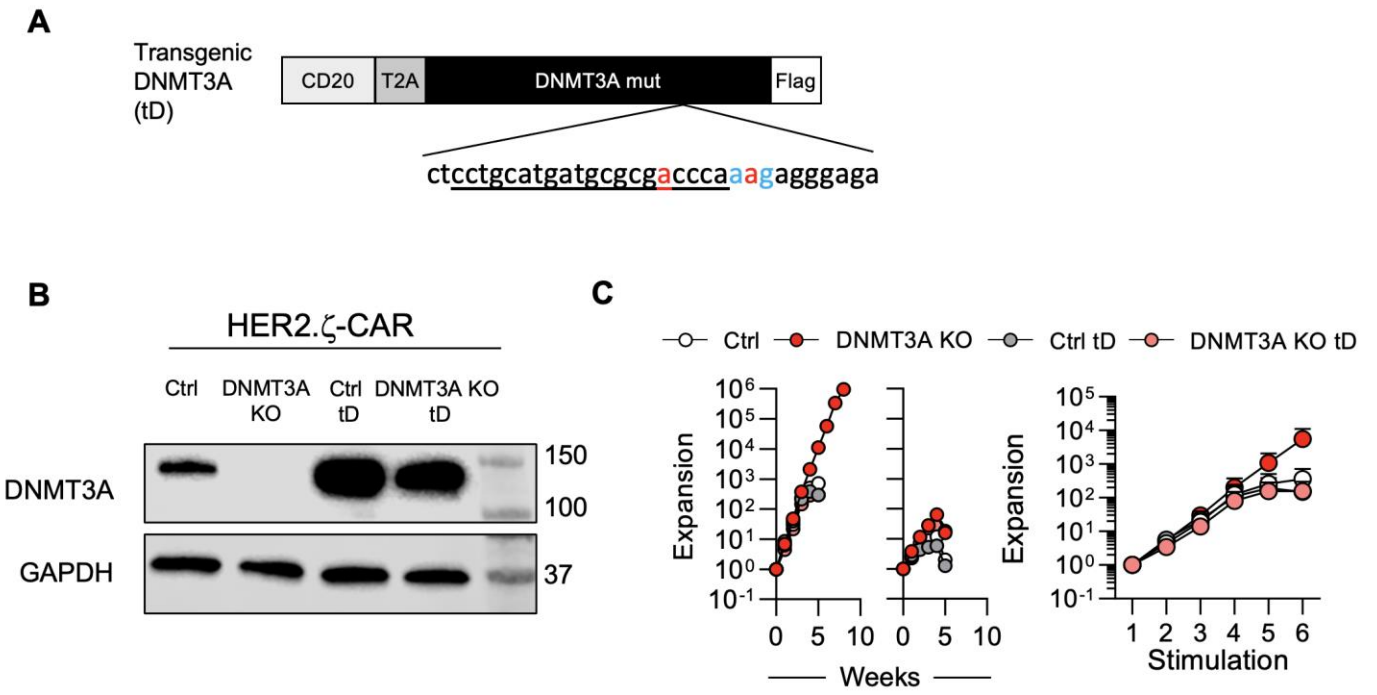

Fig. S11. Expression of transgenic DNMT3A abolishes proliferative advantage conferred by DNMT3A KO. Transgenic DNMT3A (tD) was expressed in Ctrl and DNMT3A KO HER2.ζ CAR T cells before evaluating proliferative ability. (**A**) A construct map of transgenic DNMT3A is shown. The sequence recognized by the gRNA is underlined, the PAM sequence is in blue, and the mutated nucleotides are in red. Silent mutations were chosen to prevent recognition by sgRNA and cleavage by Cas9 without changing the amino acid sequence. (**B**) Western blot was used to confirm DNMT3A expression. GAPDH was used as a loading control. (**C**) Ctrl-, DNMT3A KO-, Ctrl tD-, and DNMT3A KO tD-CAR T cells were co-cultured with U373 at a 2:1 effector:target ratio in the presence of exogenous IL-15. Cells were re-stimulated on a weekly basis with fresh tumor cells until they stopped proliferating and killing. Data are presented as mean+SEM.

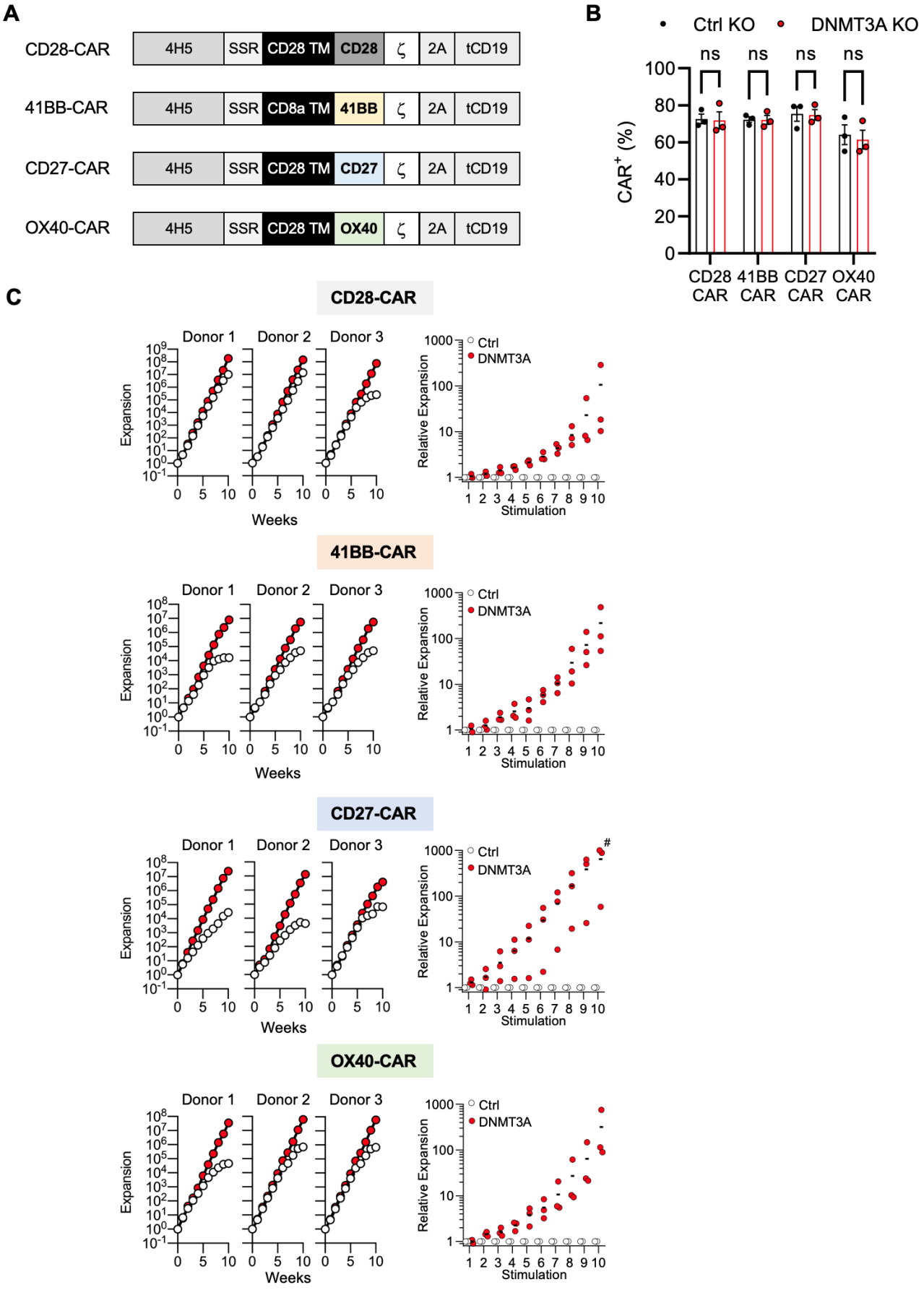

Fig. S12. DNMT3A KO improves expansion of EphA2 CAR T cells regardless of costimulatory domain. (**A**) A scheme of EphA2 CAR constructs with different costimulatory domains is shown. (**B**) CAR expression was assessed by flow cytometry at day 7 post-transduction (n=3). Data were analyzed using a two-way ANOVA with Sidak's multiple comparisons test; ns, not significant. Data are presented as mean+SEM. (**C**) EphA2 CAR T cells were used in a repeat stimulation assay against U373 with IL-15 as described in **Fig. 1C**.

T cell expansion for each donor is shown (left panels), as well as the expansion of DNMT3A KO CAR T cells relative to Ctrl KO CAR T cells at each stimulation (right panel; n=3; # indicates values set to 1000-fold to fit on graph (actual value: 3104-fold). Horizontal bars indicate mean.

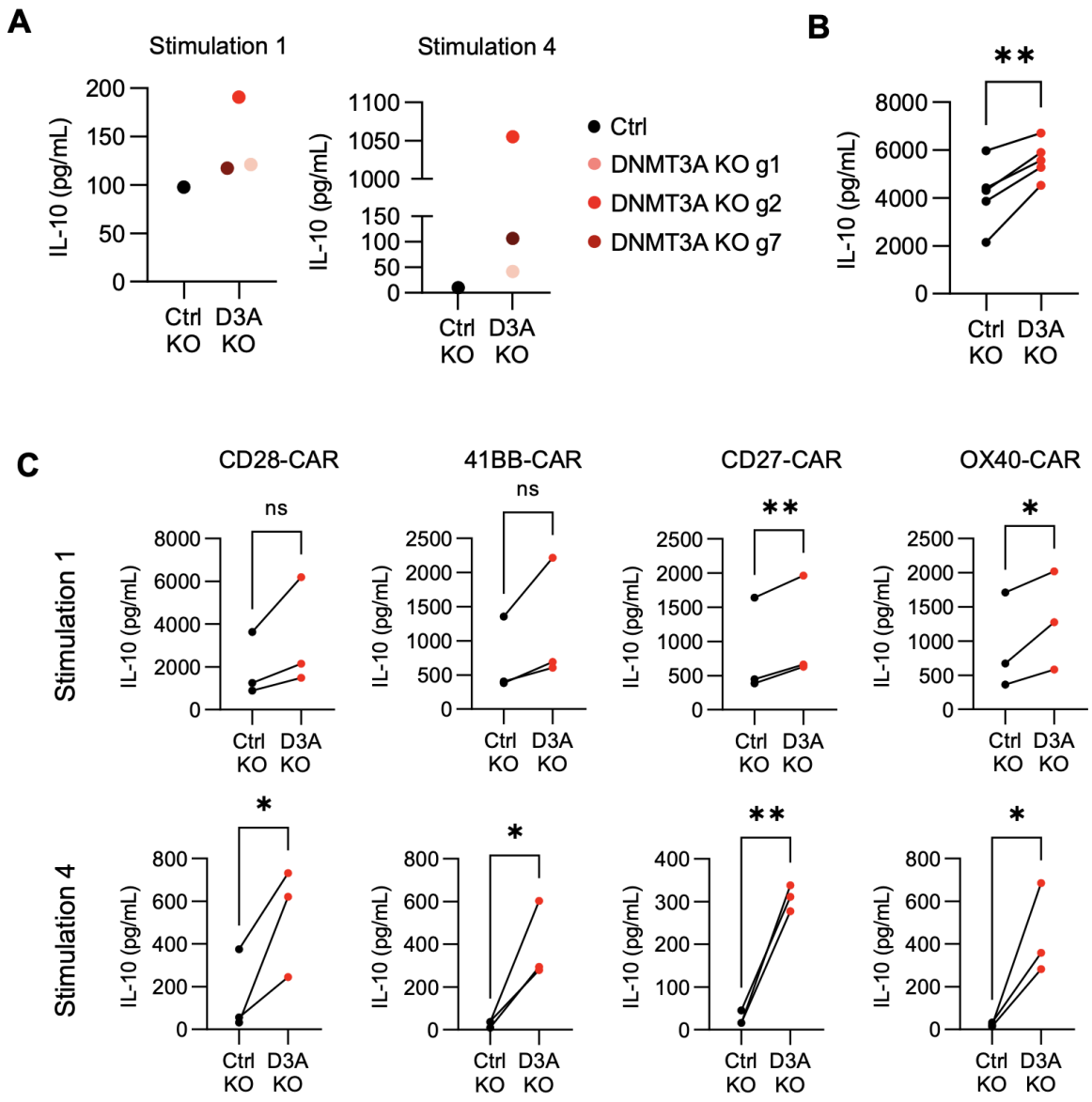

Fig. S13. DNMT3A KO CAR T cells secrete more IL-10 regardless of targeting guide, exogenous IL-15 or CAR costimulatory domain. (**A**) Ctrl or DNMT3A edited HER2.ζ CAR T cells were used in a repeat stimulation assay against U373 with IL-15 as described in **Fig. 1C**. Supernatant was collected 24 hours after the 1st and 4th stimulation with tumor cells, and a Milliplex assay was performed to assess the concentration of IL-10 (n=3). (**B**) IL13Rα2.CD28.ζ or EphA2.CD28.ζ Ctrl KO- and DNMT3A KO-CAR T cells were co-cultured with U373 tumor cells at a 2:1 ratio for 24 hours in the absence of IL-15 before supernatant was collected, and IL-10 concentration was assessed using Milliplex (n=5). (**C**) EphA2 CAR T cells with a CD28ζ, 41BBζ, CD27ζ, or OX40ζ endodomain were used in a repeat stimulation assay against U373 with IL-15 as described in **Fig. 1C**. Supernatant was collected 24 hours after the 1st and 4th stimulation with tumor cells, and a Milliplex assay was performed to assess the concentration of IL-10 (n=3). Data in B and C were analyzed by a paired one-tailed t-test; ns: not significant, *p<0.05, **p<0.01).

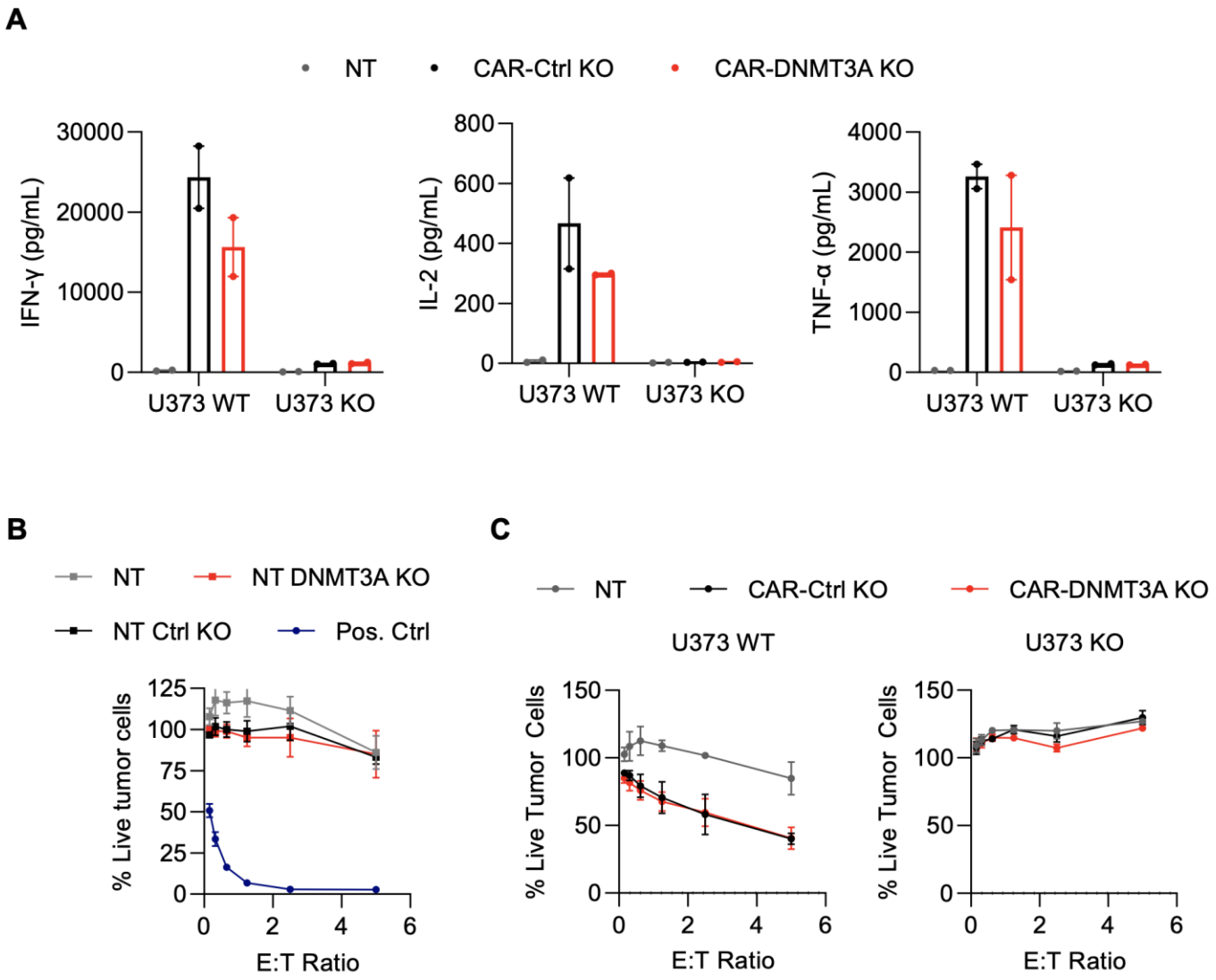

Fig. S14. Deletion of DNMT3A does not affect the antigen-dependent nature of CAR T cell cytokine production or cytotoxicity. (**A**) IL13Rα2.CD28.ζ CAR T cells were incubated with U373 WT or U373 IL13Rα2 KO tumor cells at a 2:1 ratio for 24 hours, at which time supernatant was collected. Cytokine concentrations were determined using Milliplex (n=2). Data are presented as mean±SEM. (**B and C**) T cells were incubated with U373 tumor cells with IL-15 at varying E:T ratios for 24 hours before a cell proliferation 3-(4,5-dimethylthiazol-2-yl)-5-(3-carboxymethoxyphenyl)-2-(4-sulfophenyl)-2H-tetrazolium, inner salt (MTS) assay was used to quantify remaining live tumor cells. (**B**) Non-transduced (NT) T cells or HER2.ζ CAR (Pos. Ctrl) T cells were used as effectors. U373 was used as the target cell line (n=3). Data are presented as mean±SEM. (**C**) NT or IL13Rα2.CD28.ζ CAR T cells were used as effectors. U373 WT or U373 IL13Rα2 KO were used as the target cell line (n=2). Data are presented as mean±SEM.

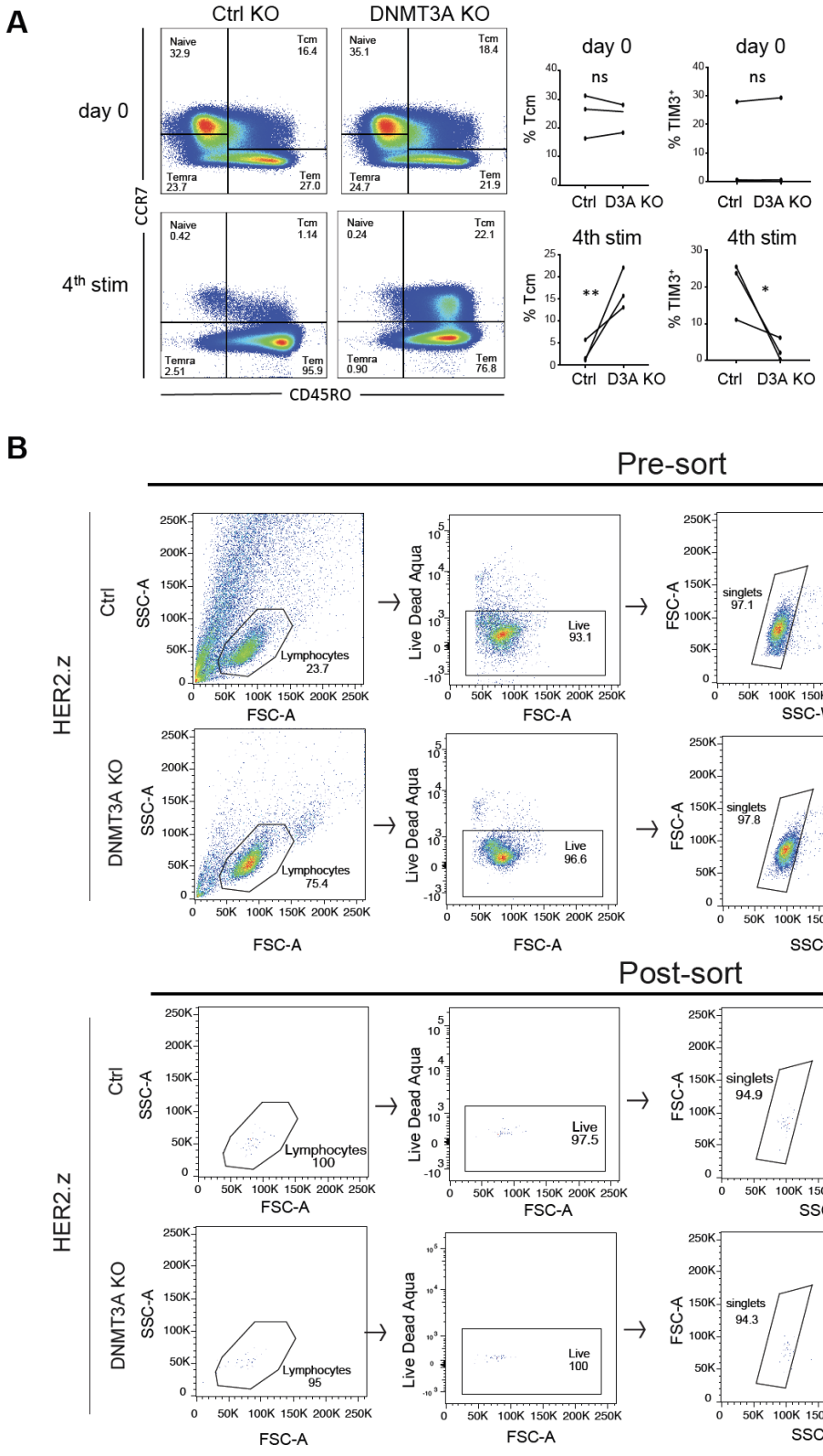

Fig. S15. Representative FACS plot of sorting technique used to isolate Ctrl and DNMT3A KO CAR T cells. (**A**) Representative FACS analysis and summary graphs of Ctrl and DNMT3A KO CAR T cells prior to and after 4 weeks of co-culture with tumor cells are shown. Data were analyzed using an unpaired t-test; *p<0.05, **p<0.01. TIM3, T cell immunoglobulin and mucin domain-containing protein 3. (**B**) Representative FACS plots show pre- and post-sort purity of Ctrl and DNMT3A KO CAR T cells used for whole genome bisulfite methylation analysis and gene expression profiling. SSC-A, side scatter area; FSC-A, forward scatter area; SSC-W, side scatter width.

A

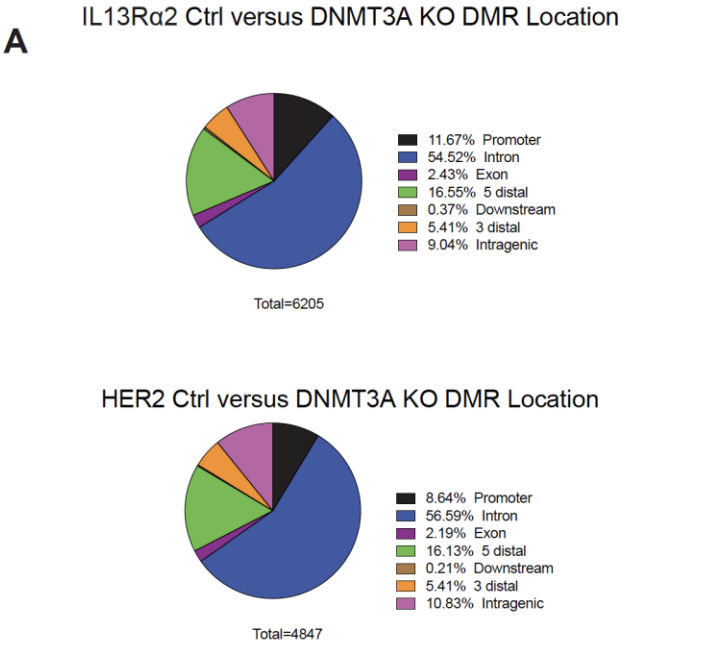

B

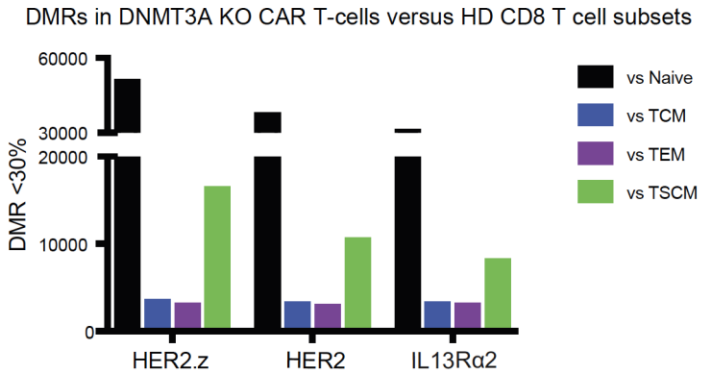

C

Ingenuity Pathway Top Upstream Regulators

Name	p-value
ID2	6.02E-17
ID3	7.21E-17
TCR	1.81E-15
CREBBP	1.09E-13
EP300	1.17E-12

D

Transcription factor upstream regulators of DNMT3A target genes

ARID5A	EGR2	GLI1	IRF8	NFKB2	RUNX3	TBX21
ATF1	EGR3	GLI2	IRF9	NFKBIB	RUVBL1	TCF12
ATF2	EIF4E	Gm21596/Hmgb1	JUN	NFYA	SATB1	TCF3
ATXN1	EIF4G2	GPS2	KAT5	NHLH2	SATB2	TCF4
BACH2	ELF1	HDAC1	KLF2	NKAP	SIRT1	TCF7
BCL11B	ELF5	HDAC2	KLF3	NKX2-1	SMAD2	TCF7L2
BCL6	ELK1	HDAC3	KLF5	NKX3-1	SMAD4	TEAD4
BCOR	ELK4	HDAC4	KLF6	NOTCH1	SMARCA4	TFAP2C
BRCA1	EOMES	HDAC6	KMT2A	NRF1	SOX11	TOX
CBFA2T3	EP300	HDAC7	LEF1	NUPR1	SOX2	TP53
CBFB	EPAS1	HES5	LYL1	PAWR	SOX9	TP63
CCND1	ERG	HESX1	MAX	PAX4	SP1	TP73
CDKN2A	ETS1	HIF1A	MDM2	PAX5	SP3	TRIM28
CDKN2C	ETV4	HIVEP2	MED1	PCGF2	SPDEF	TRPS1
CEBPA	ETV5	HLX	MED12	PML	SPI1	TRRAP
CEBPD	EZH2	Hmgb1	MEF2C	POU2AF1	SPIB	TSC22D3
CREB1	FOS	HMGB2	MEF2D	POU2F1	SQSTM1	TWIST1
CREBBP	FOXA1	HOXA3	MRTFA	POU2F2	SRF	WT1
CREM	FOXO1	HTT	MRTFB	POU4F1	STAT3	ZBED6
CTNNB1	FOXO3	ID1	MXD1	PRDM1	STAT4	ZBTB16
CYLD	FOXO4	ID2	MYB	PRDM5	STAT5A	ZBTB17
DDIT3	FOXP1	ID3	MYC	PTTG1	STAT5B	ZBTB33
DMTF1	FOXP3	IGF2BP1	MYCN	RBFOX2	STAT6	ZBTB7B
E2F1	GABPA	IKZF1	NEO1	REL	SUPT16H	ZEB2
EBF1	GATA1	IKZF2	NFATC1	RELA	TAF7L	ZFPM1
ECSIT	GATA3	IRF3	NFATC2	RRP1B	TAL1	ZNF217
EED	GFI1	IRF4	NFKB1	RUNX1	TBR1	

Fig. S16. Bioinformatic characterization of DNMT3A-mediated methylation programs. (**A**) Genome region of differentially methylated regions (DMRs) are shown between IL13Rα2 Ctrl and IL13Rα2 DNMT3A KO and HER2.CD28z Ctrl and HER2.CD28z DNMT3A KO CAR T cells. (**B**) Comparison of DMRs in DNMT3A KO CAR T cells versus healthy donor $CD8^+$ T cell subsets. (**C**) Ingenuity pathway analysis (IPA) analysis shows the top upstream regulators of DNMT3A target genes. (**D**) A table with full listing of transcription factors involved in upstream regulation of DNMT3A target genes is shown.

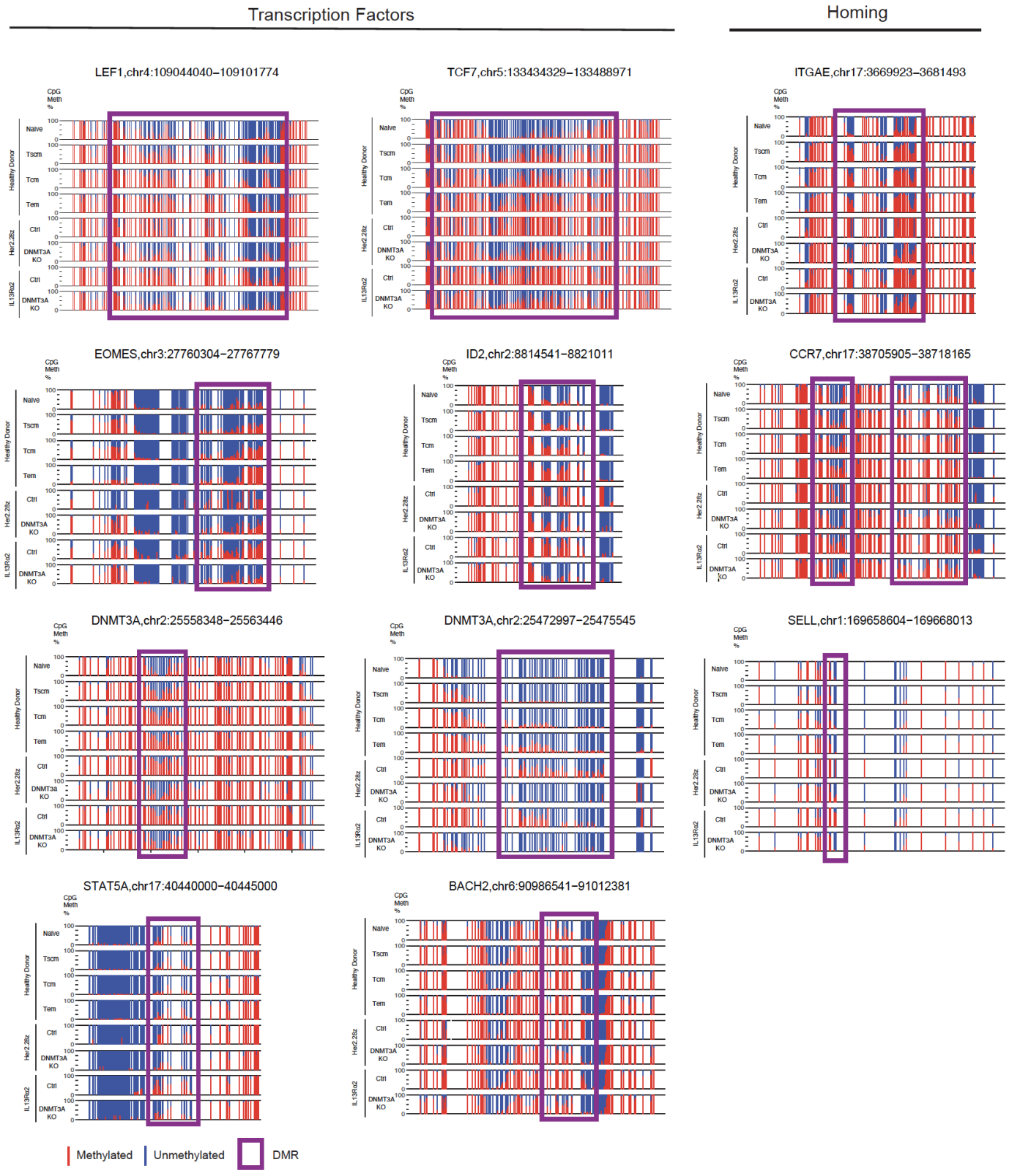

Fig. S17. DNMT3A targets transcription factors and homing loci for de novo methylation during CAR T cell exhaustion. DMRs between Ctrl and DNMT3A KO CAR T cells in transcription factors and homing loci. Individual CpG cites are represented by vertical lines with red indicating methylation and blue indicating lack of methylation. DMRs are represented by a purple box.

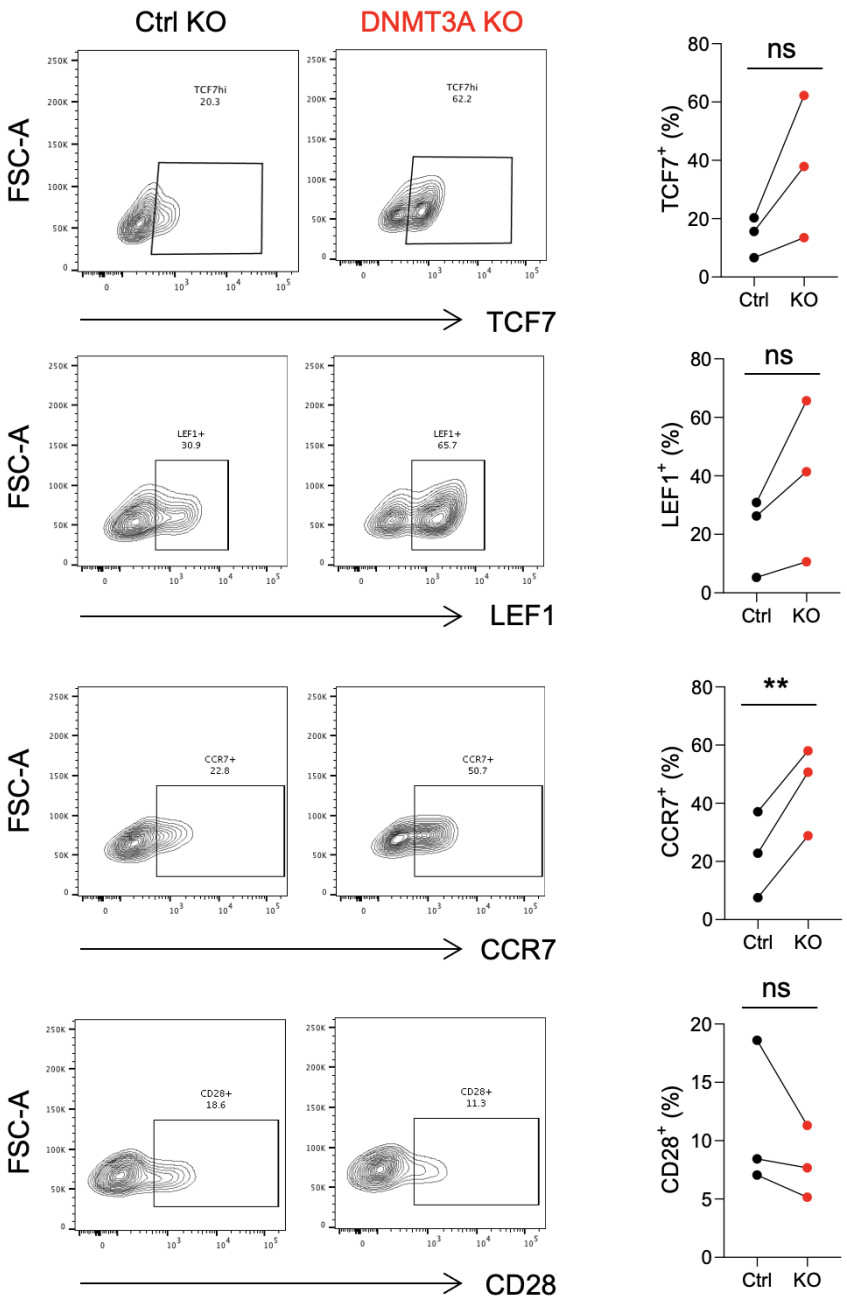

Fig. S18. DNMT3A KO CAR T cells express higher abundance of proteins associated with stemness. HER2.ζ CAR T cells were used in a repeat stimulation assay against U373 with IL-15 as described in **Fig. 1C**. 24 hours after the 4th stimulation, expression of TCF7, LEF1, CCR7, and CD28 was assessed using flow cytometry. Representative flow plots and summary data are shown (n=3). Data were analyzed using paired t-tests; ns: not significant, **p<0.01.

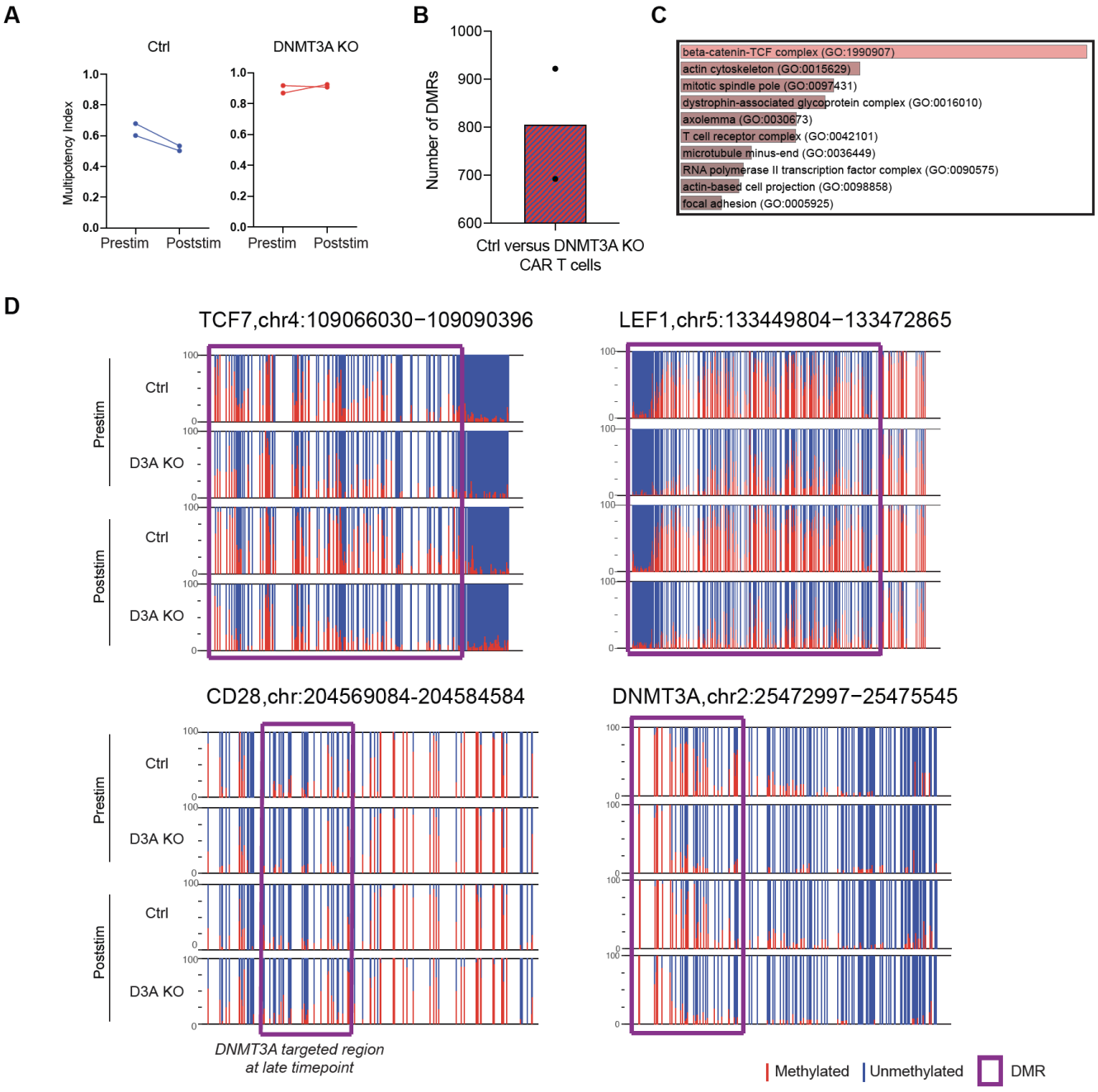

Fig. S19. DNMT3A-mediated de novo methylation of CAR T cells occurs both before and after antigen exposure. (**A**) Multipotency index scores comparing Ctrl and DNMT3A KO CAR T cells pre and post exposure to daily tumor stimulation (stim) are shown. (**B**) The number of DMRs between Ctrl and DNMT3A KO CAR T cells after four days of continuous in vitro tumor exposure is shown. (**C**) Gene ontology of biological processes regulated by DNMT3A are shown. P-values are based on Fisher's Exact Test. (**D**) Representative gene loci (TCF7, LEF1, CD28, DNMT3A) of Ctrl and DNMT3A KO CAR T cells are shown. Red indicates methylated CpG and blue indicates unmethylated CpG. The purple boxes highlights DMRs. The purple box presented in the plot for CD28 represents an experimentally determined DNMT3A-targeted region that has not yet undergone de novo methylation in this experiment.

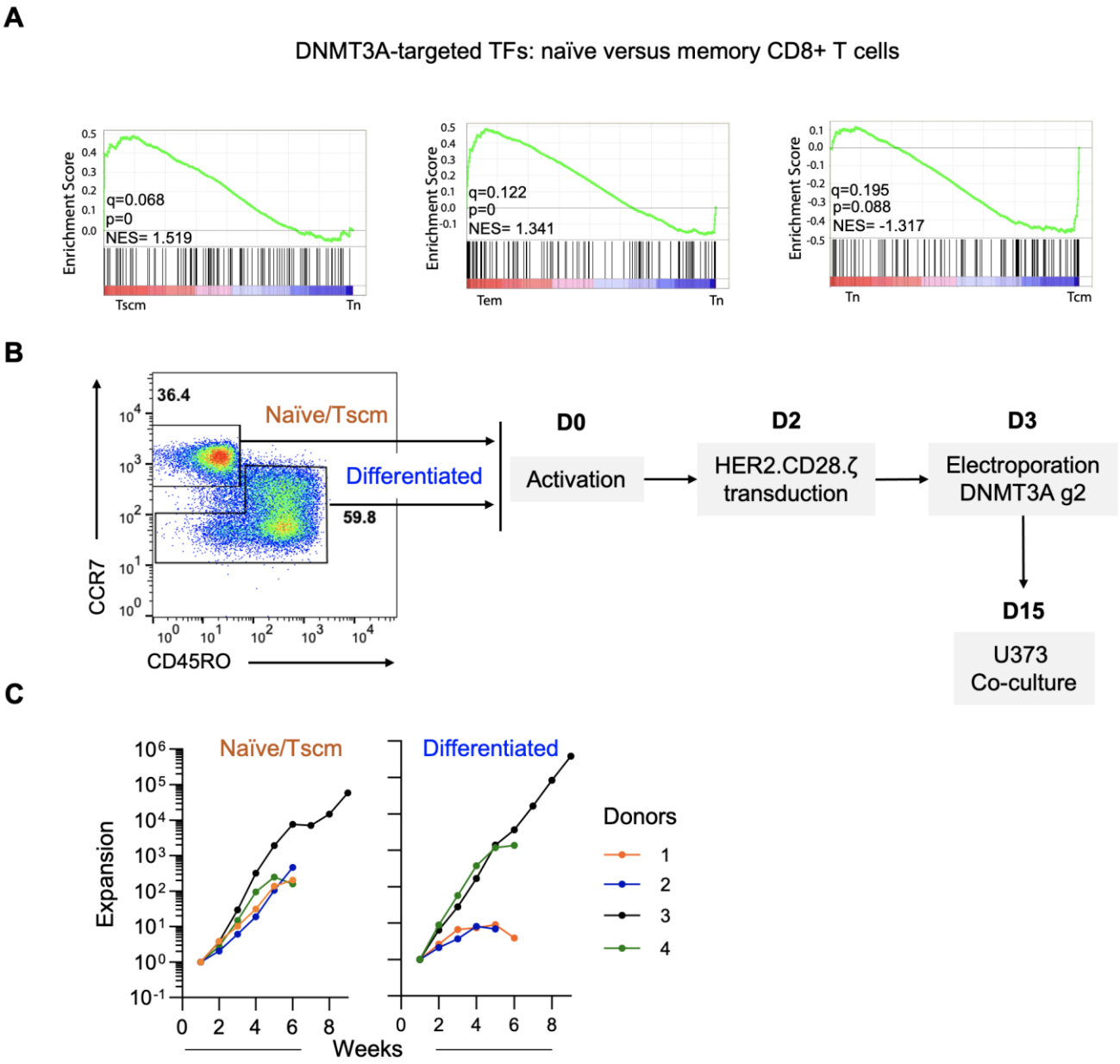

Fig. S20. DNMT3A deletion promotes selective survival of human T cell subsets that have high multipotent differentiation potential. (**A**) Gene set enrichment analysis (GSEA) of DNMT3A-targeted transcription factors among human naïve and memory CD8$^+$ T cell subsets are shown. (**B**) Schematic representation of the sorting procedure used to isolate naïve/Tscm and differentiated CD8$^+$ T cell subsets with subsequent generation of subsetted DNMT3A KO CAR T cells. (**C**) Expansion of naïve/Tscm and differentiated CAR T cell subsets in the repeat stimulation assay is shown (n=4 donors).

A

IL-10 Mediated Gene Expression is Enriched for DNMT3A targets

DNMT3A target	Non DNMT3A target	Fisher's Exact Test	Odds ratio
7	25	p=0.0035	4.114

* Among total of ~13,500 measurable gene expression events from Affymetrix dataset GSE79127

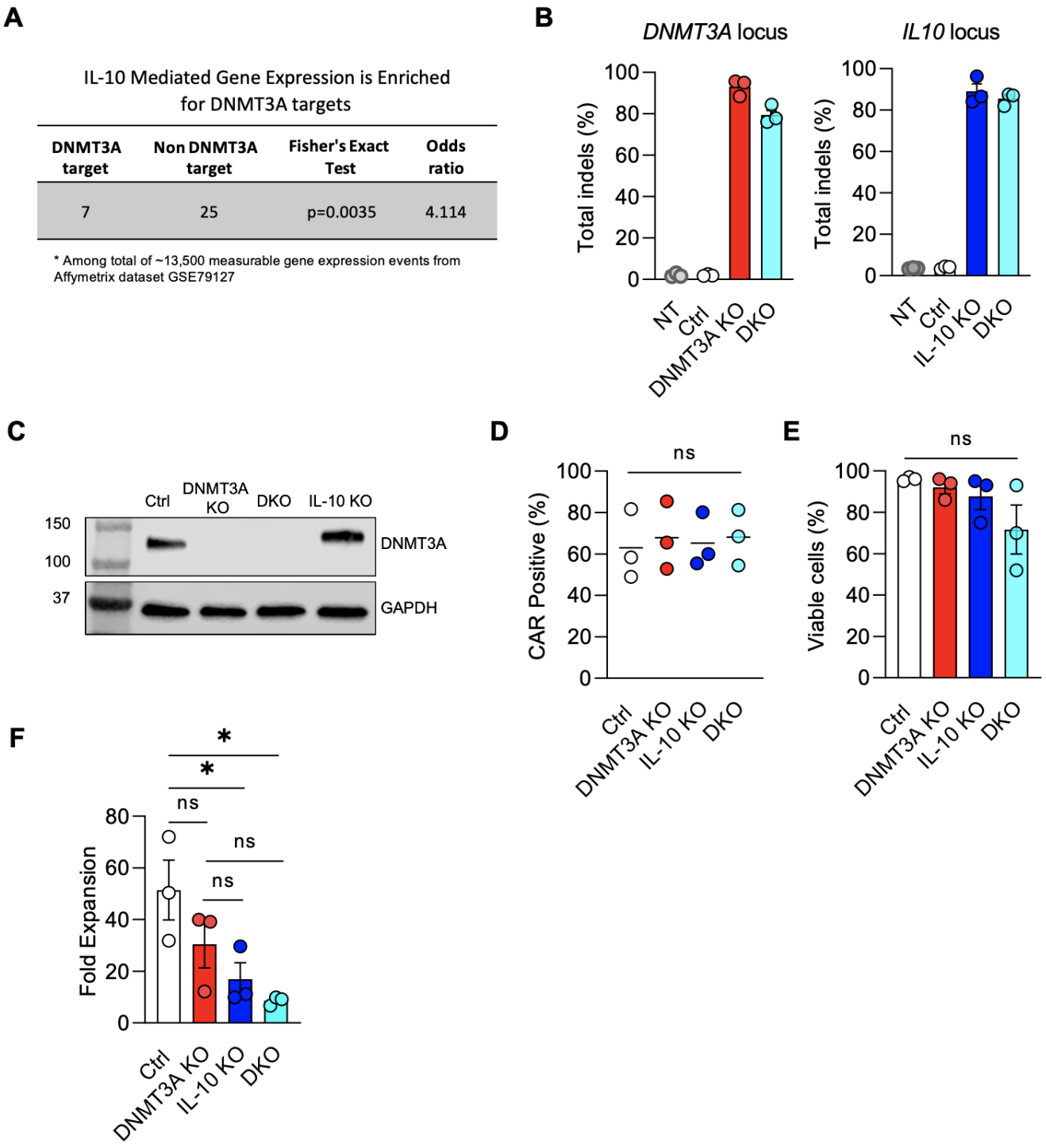

Fig. S21. IL-10 KO in DNMT3A edited CAR T cells. (**A**) The table shows expression of genes upregulated by IL-10 that overlap with DNMT3A targets. (**B**) Targeted NGS data evaluating indels at the *DMNT3A* and *IL10* loci are shown for the indicated CAR T cell populations. Data are presented as mean±SEM. (**C**) A western blot confirming DNMT3A knock-out is shown; GAPDH served as the loading control. (**D**) CAR transduction efficacy in gene edited CAR T cells was measured. Horizontal bars indicate mean. (**E**) Gene edited CAR T cell viability at day 8 to 10 post transduction is shown. Data are presented as mean±SEM. (**F**) Gene edited CAR T cell expansion over 10 days in culture are shown. Data are presented as mean±SEM. NT indicates non-transduced T cells, Ctrl indicates T cells transduced with double control guides to mimic double KO conditions; DNMT3A KO and IL-10 KO indicates single knock-out conditions; DKO indicates DNMT3A and IL-10 double knock-out (N=3 per group). Data were analyzed with a two-way ANOVA with Tukey's multiple comparisons test; *p<0.05, ns: not significant.

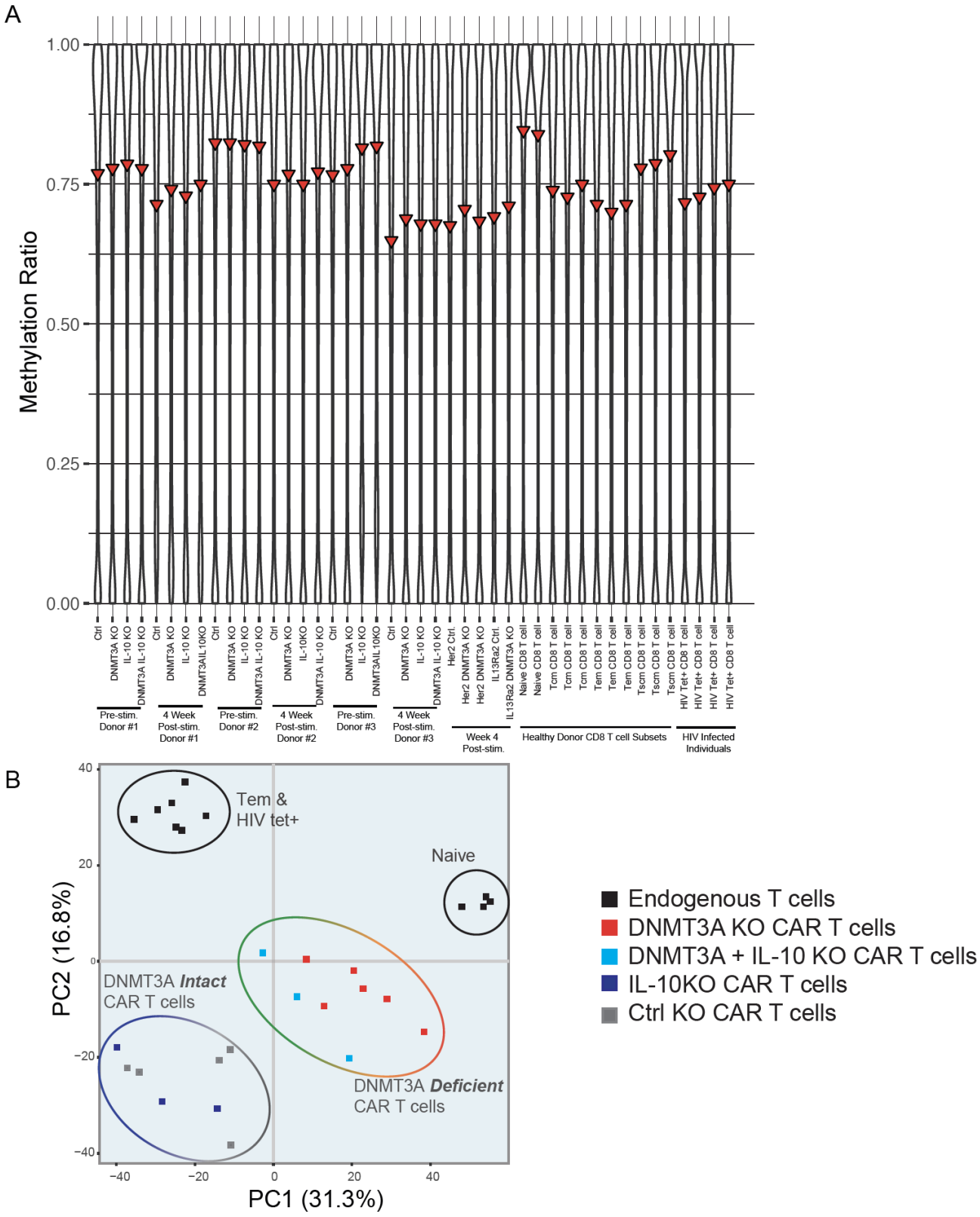

Fig. S22. Genome wide comparison of Ctrl and DNMT3A KO CAR T cells with function and exhausted endogenous CD8⁺ T cell populations. (**A**) Violin plot characterizing the methylation ratio of Control (Ctrl) KO, DNMT3A KO, IL-10 KO, and DNMT3A + IL-10 (DKO) CAR T cells from three separate donors are shown as comported to CD8⁺ T cell subsets from healthy human donors and tetramer positive (tet⁺) CD8⁺ T cells from human immunodeficiency virus (HIV) infected individuals. Red arrows indicate mean methylation values. (**B**) Principal component analysis (PCA) of whole genome methylation profiles showing segregation of week 4 post-stimulation DNMT3A-deficient CAR T cells from CAR T cells with intact DNMT3A activity.

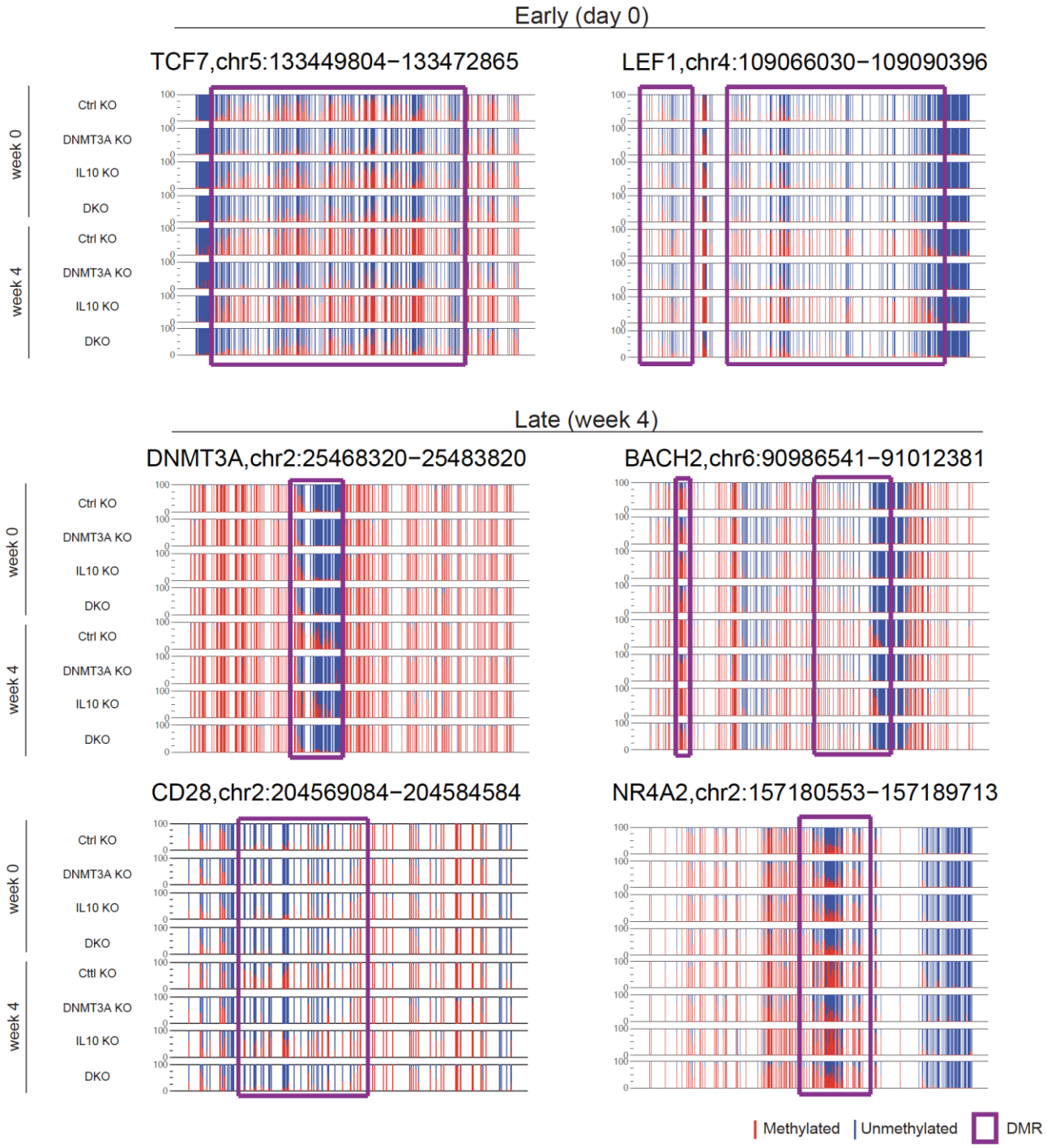

Fig. S23. DNMT3A-mediated methylation programming occurs both early and late during chronic antigen stimulation. DMRs between control (Ctrl) KO, DNMT3A KO, IL-10 KO, and DNMT3A + IL-10 double KO (DKO) CAR T cells at week 0 and week 4 post-stimulation are shown. Individual CpG sites are represented by vertical lines with red indicating methylation and blue indicating lack of methylation. DMRs are represented by a purple box.

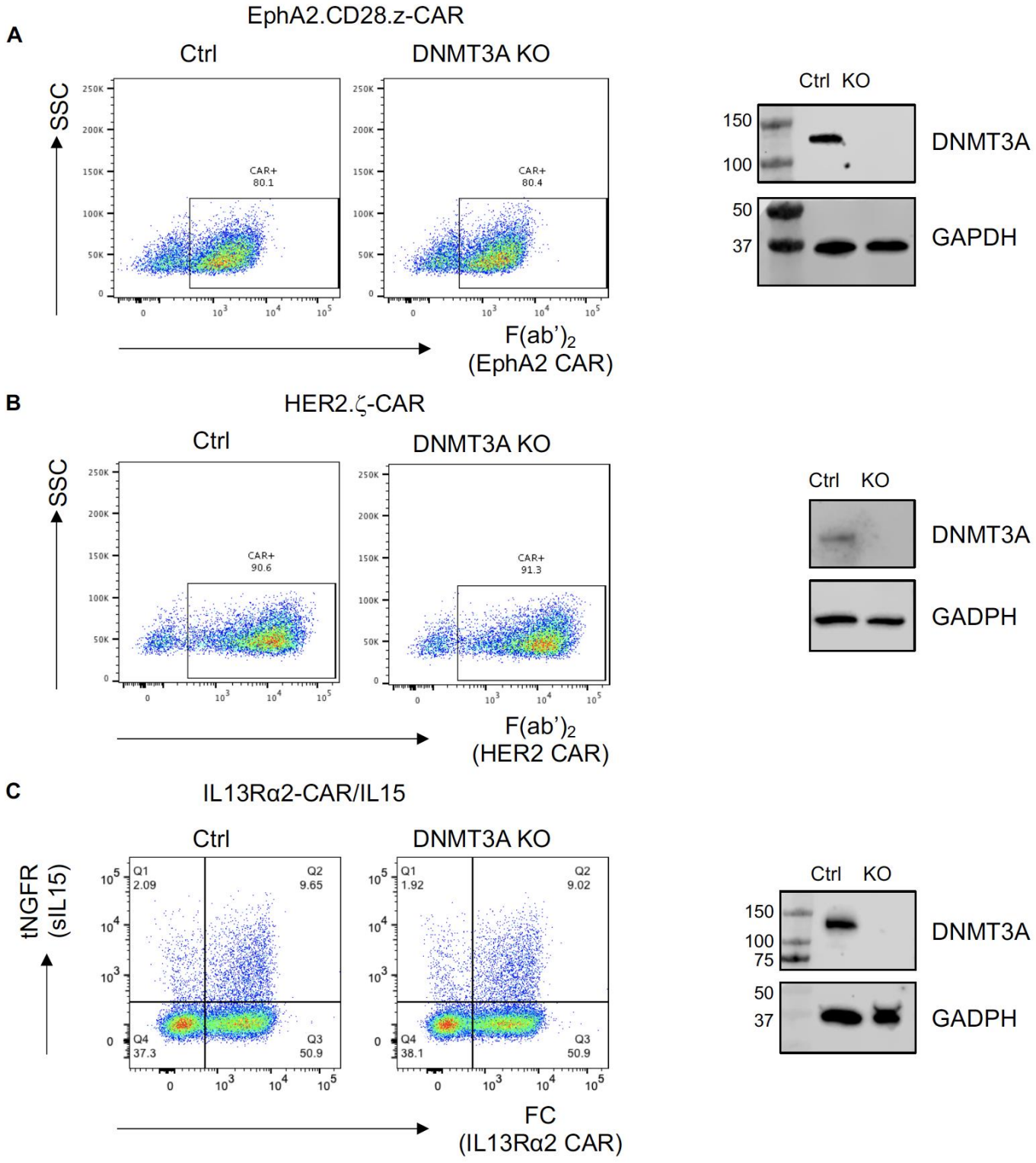

Fig. S24. CAR expression and DNMT3A KO efficiency in CAR T cells used for in vivo experiments. Flow cytometry was used to detect CAR expression of Ctrl and DNMT3A KO CAR T cells and western blot was used to confirm DNMT3A KO; GAPDH was used as a loading control. (**A**) Data are shown for EphA2-CAR T cells used in **Fig. 5A to C**. (**B**) Data are shown for HER2.ζ-CAR T cells used in **Fig. 5D to F**. (**C**) I Data are shown for L13Rα2-CAR T cells used in **Fig. 5G to I** and **fig. S26**.

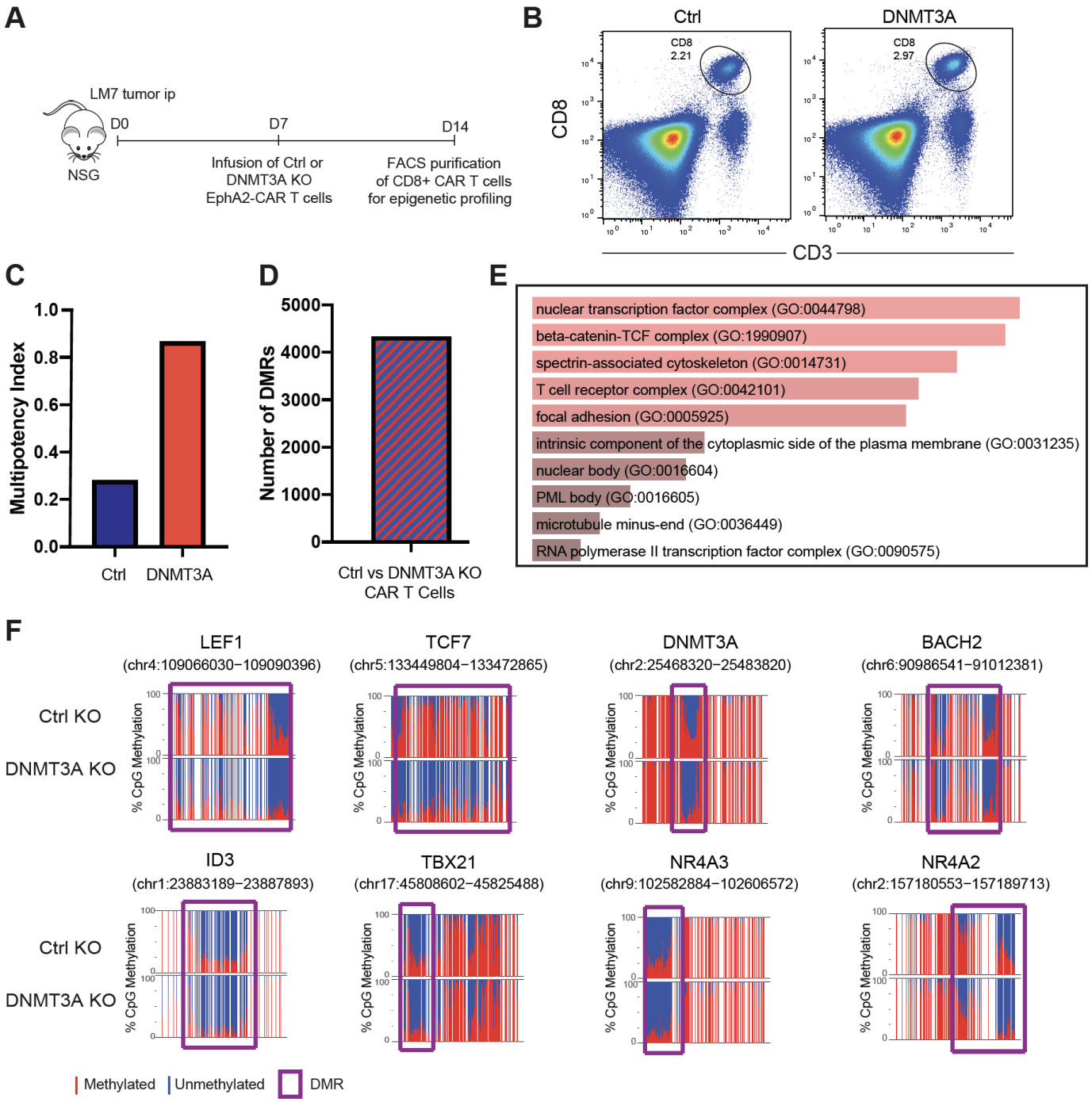

Fig. S25. DNMT3A targets stem-associated loci during in vivo CAR T cell anti-tumor response. (**A**) Experimental setup showing injection of Ctrl or DNMT3A KO EphA2-CAR T cells into tumor-bearing NOD scid gamma (NSG) mice. (**B**) Representative FACS plot show Ctrl and DNMT3A KO CAR T cells isolated from mice one week after injection. (**C**) Multipotency index score comparing Ctrl and DNMT3A KO CAR T cells pre and post exposure to in vivo tumor antigen for one week is shown. (**D**) The number of DMRs between Ctrl and DNMT3A KO CAR T cells after one week of in vivo tumor exposure is shown. (**E**) Gene ontology of biological processes regulated by DNMT3A are shown. (**F**) Representative methylation profiles of gene loci among Ctrl and DNMT3A KO CAR T cells isolated after one week of in vivo tumor exposure are shown. Red is methylated CpG, Blue is unmethylated CpG. The purple boxes highlight DMRs.

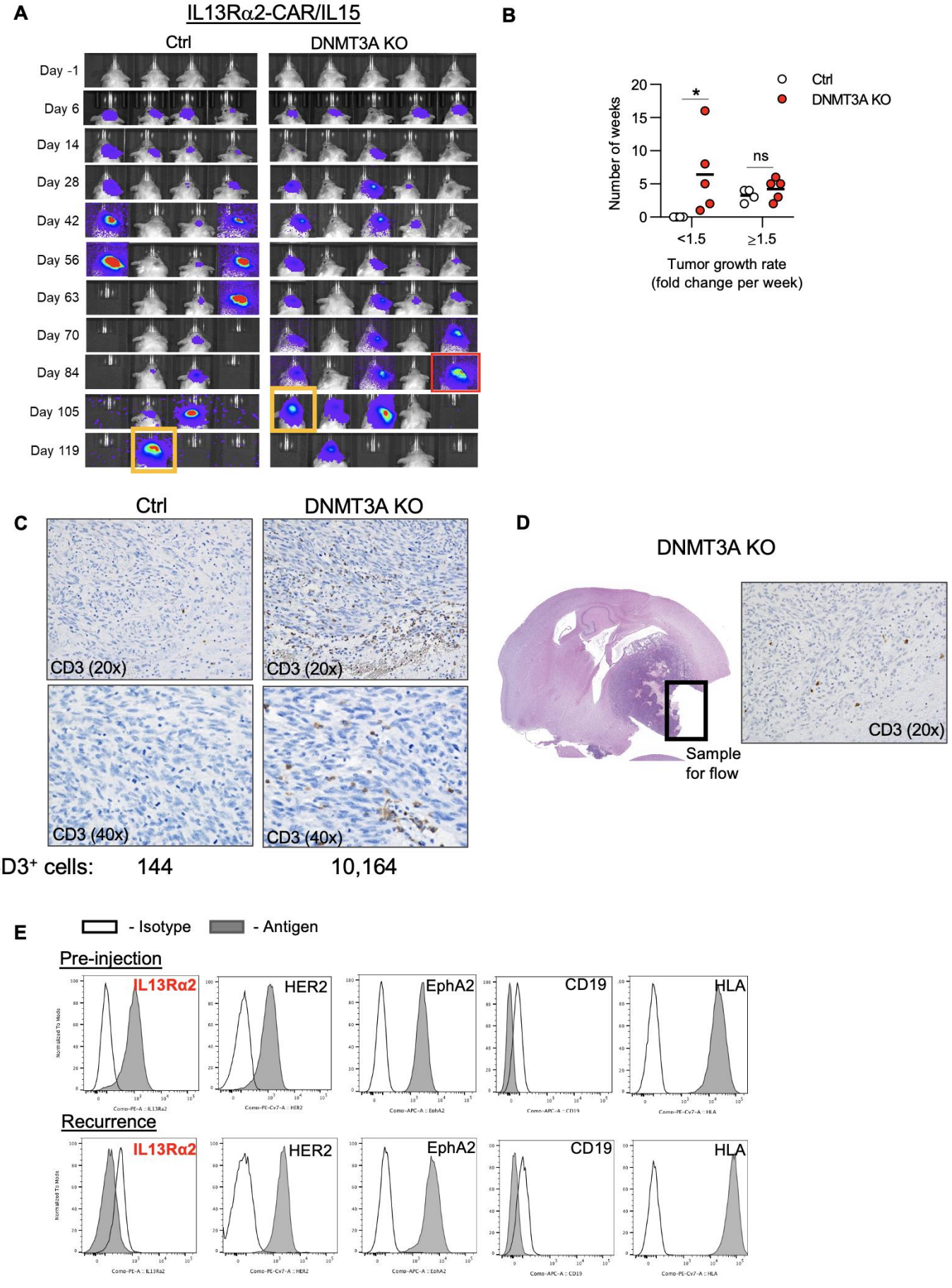

Fig. S26. Analysis of recurrent tumors reveals antigen-negative relapse and long-term persistence of DNMT3A KO CAR T cells. (**A**) Bioluminescence images of the intracranial glioma model described in Fig. 5G to I. Gold squares indicate the mice used for immunohistochemistry (IHC, panel C). Red square indicates the mouse whose tumor was used for IHC (panel D) and flow cytometry (panel E). (**B**) After initial progression

(defined as a greater than 4-fold increase in total flux between consecutive measurements), tumor growth rates were calculated by dividing consecutive total flux data points. The number of weeks tumors grew slowly (flux increase less than 1.5-fold) or rapidly (flux increase greater than 1.5-fold) are shown for each mouse. Horizontal bars indicate mean. Data were analyzed using Mann-Whitney tests with two-stage step-up Benjamini, Krieger, & Yekutieli False Discovery Rate procedure; ns: not significant, *$p<0.05$. (**C**) IHC for human CD3 in recurrent tumors removed from mice treated with Ctrl or DNMT3A KO CAR T cells greater than 100 days post tumor injection is shown. $CD3^+$ numbers indicate $CD3^+$ human T cells within the tumor quantified using Indica Labs – CytoNuclear v2.0.9 analysis module. Ctrl is from a sample collected on day 119 post-tumor injection; DNMT3A KO indicates a sample collected on day 105 post-tumor injection. The mice are indicated by gold squares in (A). (**D**) Hematoxylin and eosin (H&E) stain (left) and IHC for human CD3 (right) of a recurrent tumor that was also used for flow cytometric analysis of surface antigen expression is shown. (**E**) Flow cytometry for tumor associated antigens, CD19 (negative control), and human leukocyte antigen (HLA, positive control) on U373 pre-injection and recurrent U373 taken from DNMT3A KO group is shown (Day 84, mouse indicated by red square in Panel A).

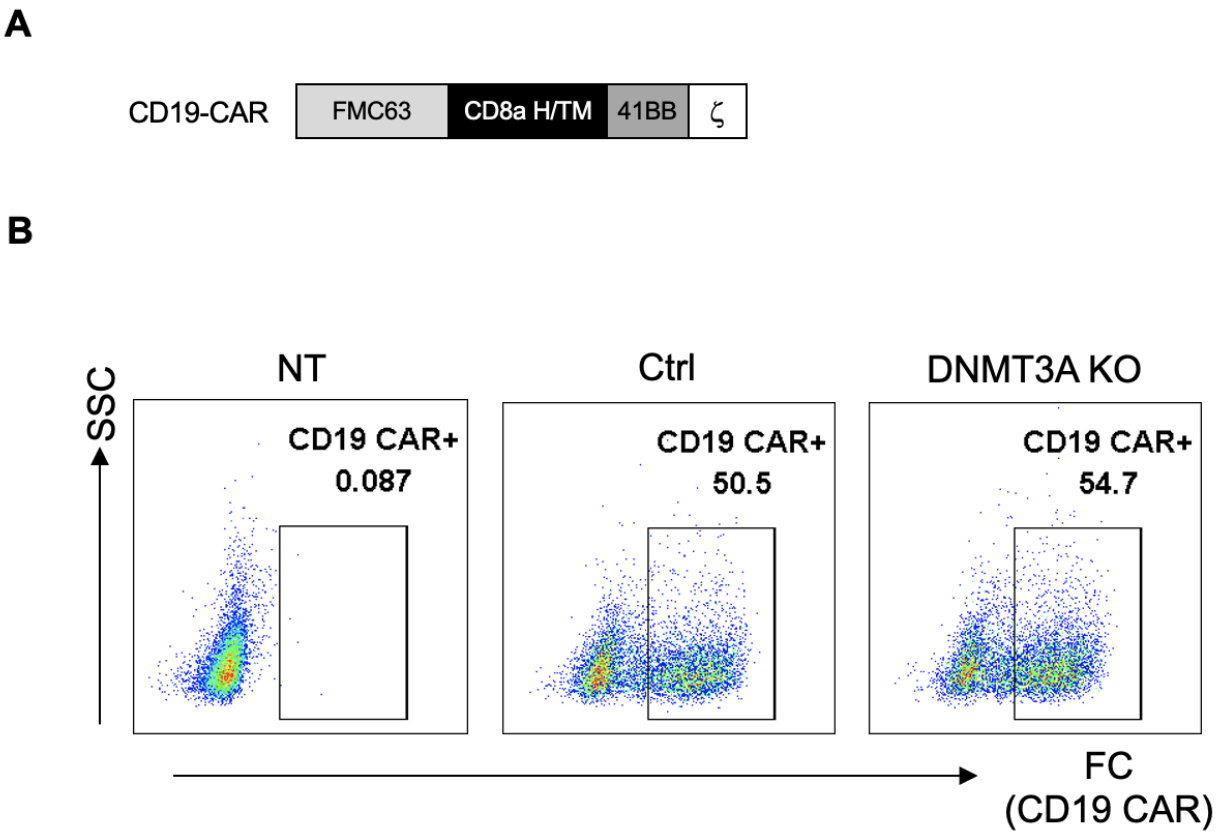

Fig. S27. CD19-CAR T cells used for in vivo experiments. (**A**) Scheme of CD19-specific CAR lentiviral vector as described in (61). H/TM: hinge and transmembrane domain. (**B**) Flow cytometry of CAR expression on Ctrl and DNMT3A KO CD19-CAR T cells used in **Fig. 6A to D** is shown.

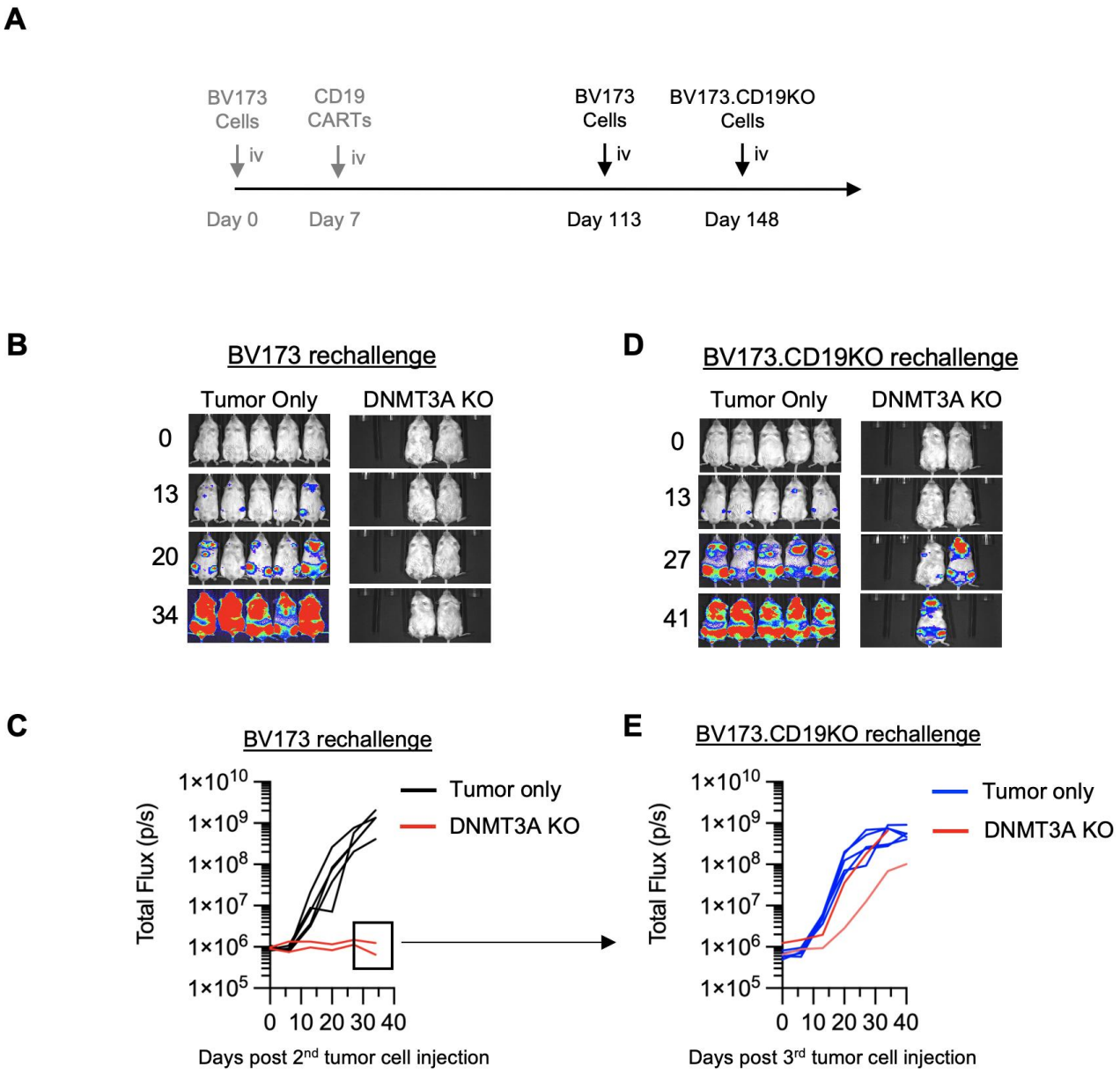

Fig. S28. Rechallenge in vivo experiment demonstrates the functional persistence of DNMT3A KO CD19-CAR T cells. (**A**) Scheme of rechallenge experiment. DNMT3A KO CD19-CAR T cell-treated NSG mice that completely responded to the T cell therapy (n=2) were injected with a second intravenous (iv) dose of $3x10^6$ BV173-ffLuc tumor cells on Day 113 post initial tumor implantation. At day 148, surviving DNMT3A KO CD19-CAR treated animals (n=2) were then injected iv with $3x10^6$ BV173.CD19KO-ffLuc tumor cells. For both tumor rechallenge experiments, naïve, age-matched mice were injected with tumor cells to demonstrate tumor engraftment (tumor only) (**B**) Representative bioluminescence images of each treatment group are shown. (**C**) Quantitative bioluminescence imaging (total flux) data for each mouse in panel B are shown. Black box indicates animals used for the BV173.CD19KO rechallenge experiment. (**D**) Representative bioluminescence images of each treatment group of the BV173.CD19KO rechallenge experiment are shown. (**E**) Quantitative bioluminescence imaging (total flux) data for each mouse is shown.

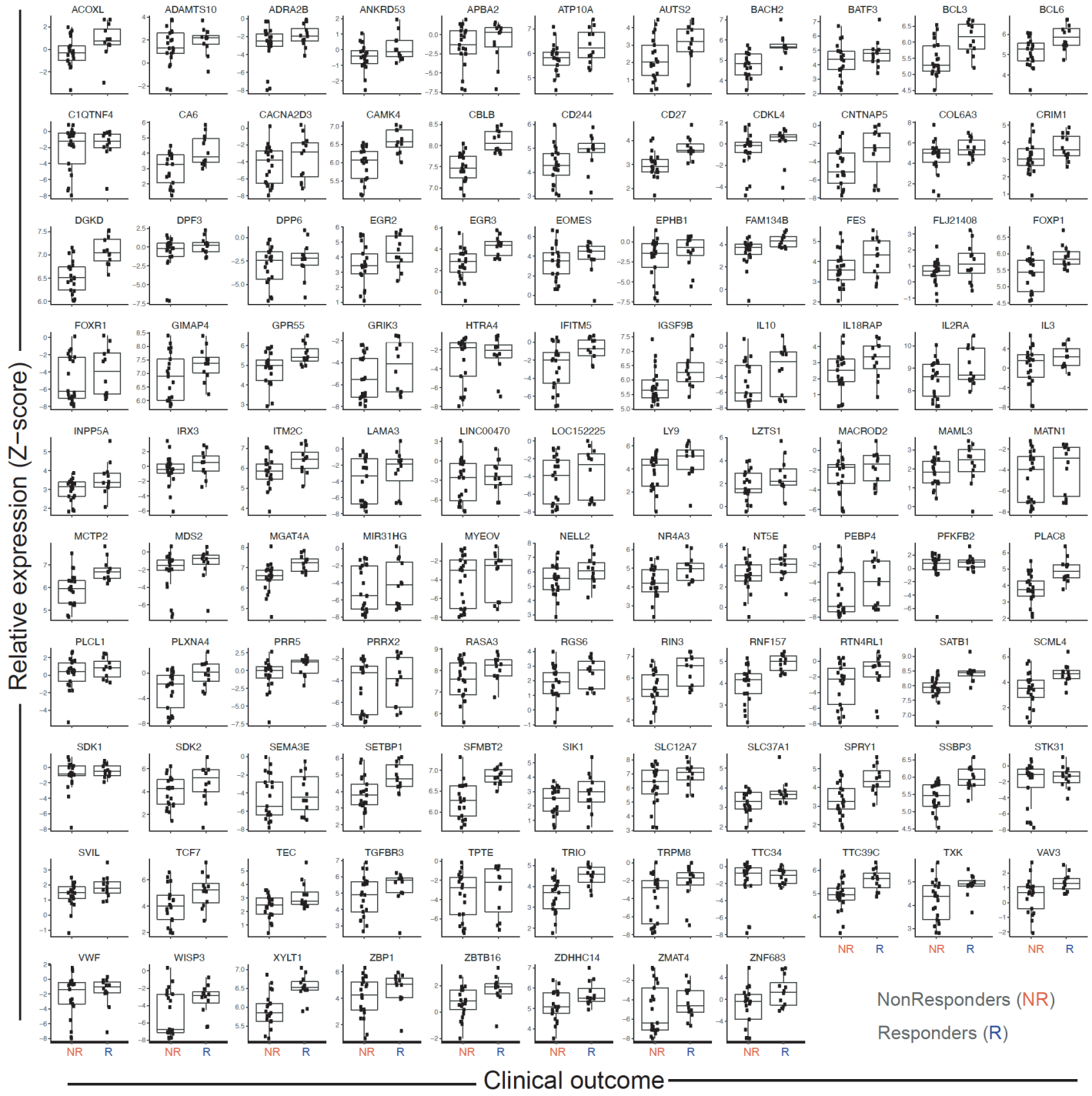

Fig. S29. Individual DNMT3A target gene expression from CD19 CAR T-cell CLL product. Relative expression of individual DNMT3A signature genes. The lower and upper hinges correspond to the first and third quartiles (the 25th and 75th percentiles). The upper whisker extends from the hinge to the largest value no further than 1.5 * IQR from the hinge. The lower whisker extends from the hinge to the smallest value at most 1.5 * IQR of the hinge. IQR, inter-quartile range, or distance between the first and third quartiles).

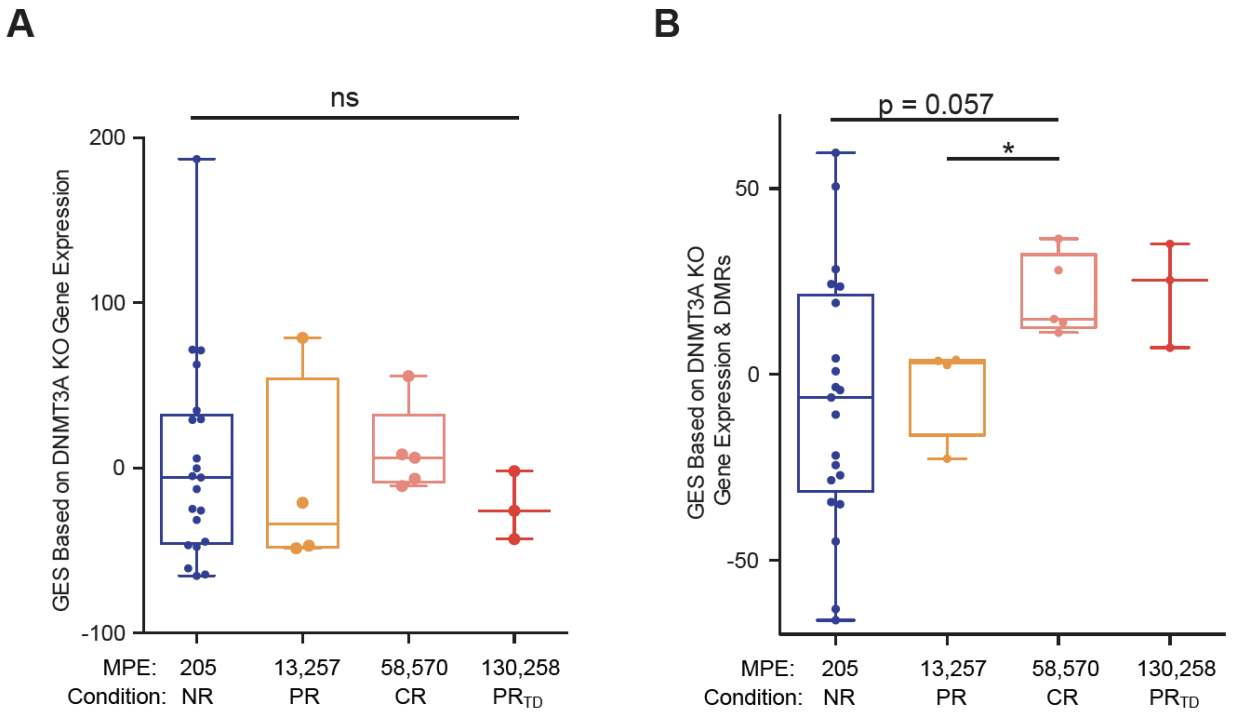

Fig. S30. Gene expression indirectly regulated by DNMT3A cannot solely predict clinical response in patients treated with CD19-CAR T cell therapy for CLL. (**A**) A summary graph is shown based solely on DNMT3A gene expression in the CAR T cell product of responders (CR, PR, PRTD) versus non-responders to CD19-CAR T cell therapy for CLL. NR: no response, CR: complete response, PR: partial response, PR_{TD}: PR followed by relapse with transformed B cell lymphoma. (**B**) CAR T cell product gene expression scores are shown for DNMT3A target genes in the context of the DNMT3A DMR list comparing responders (CR, PR, PRTD) and non-responders. Statistical significance was determined by a Mann-Whitney test. Error bars are defined based on the minimum and maximum quartile, *p<0.05, **p<0.01. Publicly available data set (47) was used for analysis. MPE, median peak expansion.

Table S1. **Protospacer and primer sequences**. Table contains single guide RNA sequences and sequencing primers used in the study.

Gene	Protospacer	Primers
IL10	5’ GTTGTTAAAGGAGTCCTTGCNGG 3’	F – 5’ GGTCCCATCACTGTTGAATCCTCTGT 3’ R – 5’ ACCCTCTGGCTGCTGGATGTGCTGA 3’
DNMT3A	g1 - 5’ TGGCGCTCCTCCTTGCCACGNGG 3’	F – 5’ TCCCGATGACCCTGTCTTCCCGTGC 3’ R – 5’ AGGTAGAAGCCATTAGTGAGCTGGC 3’
	g2 - 5’ CCTGCATGATGCGCGGCCCANGG 3’	
	g3 - 5’ GCATGATGCGCGGCCCAAGGNGG 3	
	g7 - 5’ CAGCACCACGGCACGGAAGGNGG 3	
mCherry	g17-5’ CAAGTAGTCGGGGATGTCGGNGG 3’	
	g19-5’ AGTAGTCGGGATGTCGGCGNGG 3’	